International Journal of Nanomedicine

Dovepress

open access to scientific and medical research

Open Access Full Text Article

ORIGINAL RESEARCH

PEGylated SLN as a Promising Approach for Lymphatic Delivery of Gefitinib to Lung Cancer

Abdelrahman Y Sherif[1,2], Gamaleldin I Harisa[1–3], Fars K Alanazi[1,2], Fahd A Nasr[4], Ali S Alqahtani[4]

[1]Kayyali Chair for Pharmaceutical Industry, College of Pharmacy, King Saud University, Riyadh, Saudi Arabia; [2]Department of Pharmaceutics, College of Pharmacy, King Saud University, Riyadh, Saudi Arabia; [3]Department of Biochemistry and Molecular Biology, College of Pharmacy, Al-Azhar University, Nasr City, Cairo, Egypt; [4]Department of Pharmacognosy, College of Pharmacy, King Saud University, Riyadh, Saudi Arabia

Correspondence: Abdelrahman Y Sherif, Tel +966 500859725, Email ashreef@ksu.edu.sa

Purpose: The present study aimed to develop gefitinib-loaded solid lipid nanoparticles (GEF-SLN), and GEF-loaded PEGylated SLN (GEF-P-SLN) for targeting metastatic lung cancer through the lymphatic system.

Methods: The prepared SLNs were characterized in terms of physicochemical properties, entrapment efficiency, and in-vitro release. Furthermore, ex-vivo permeability was investigated using the rabbit intestine. Cytotoxicity and apoptotic effects were studied against A549 cell lines as a model for lung cancer.

Results: The present results revealed that the particle size and polydispersity index of the prepared formulations range from 114 to 310 nm and 0.066 to 0.350, respectively, with negative zeta-potential (−14 to −27.6). Additionally, SLN and P-SLN showed remarkable entrapment efficiency above 89% and exhibited sustained-release profiles. The permeability study showed that GEF-SLN and GEF-P-SLN enhanced the permeability of GEF by 1.71 and 2.64-fold, respectively, compared with GEF suspension. Cytotoxicity showed that IC_{50} of pure GEF was 3.5 µg/mL, which decreased to 1.95 and 1.8 µg/mL for GEF-SLN and GEF-P-SLN, respectively. Finally, the apoptotic study revealed that GEF-P-SLN decreased the number of living cells from 49.47 to 3.43 when compared with pure GEF.

Conclusion: These results concluded that GEF-P-SLN is a promising approach to improving the therapeutic outcomes of GEF in the treatment of metastatic lung cancer.

Keywords: solid lipid nanoparticles, PEGylated SLN, intestinal permeability, gefitinib, cytotoxicity, apoptosis

Introduction

Lung cancer represents a life-threatening problem globally where it is the second most common type of cancer worldwide.[1] The primary cause of death in all types of cancer resulted from cancer metastasis.[1] Cigarette smoking is the biggest risk factor for the development of lung cancer that is exaggerated in the presence of alcohol drinking.[2] Additionally, exposure to arsenic, radon, asbestos, radiation, air pollution, and tuberculosis increases the development of lung cancer. Moreover, smoking and alcohol drinking worsen the family history of developing lung cancer.[3] The lymphatic system (LS) is one of the gateways for the metastasis of cancer cells. In this context, cancer cells are regularly detached from the primary tumor site through the LS and escape inside the lymph nodes.[4] Unfortunately, escaped cancer cells within the lymph nodes are considered a primary source of cancer relapse after the completion of treatment.[5] Therefore, lymphatic drug delivery (LDD) is a promising approach in the treatment of cancer and prevents cancer relapse.[5]

LDD could be achieved via different routes including oral administration. The oral route is characterized by simplicity, painlessness, avoiding the need for hospitalization, and training a person.[4] Physiologically, the LS plays a fundamental role in the absorption of large particles and dietary molecules including lipids, lipophilic vitamins, and lipophilic drugs.[6] Herein, LDD could be achieved by assembling drug cargoes to take the same track of chylomicrons in the endoplasmic reticulum of the enterocytes or absorption through M cells.[4] Orally administered drugs are usually absorbed via the portal vein and exposed to hepatic first-pass metabolism that decreases drug bioavailability.[5] In contrast,

Received: 16 March 2022
Accepted: 6 July 2022
Published: 28 July 2022

Graphical Abstract

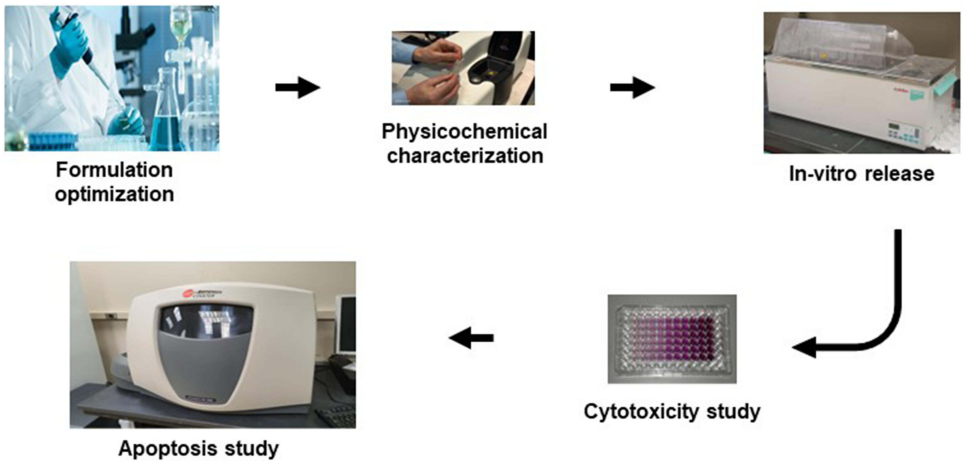

the oral dosage forms planned for the LDD could evade hepatic first-pass metabolism and enhance drug bioavailability.[4] In this regard, different types of lipid-based drug delivery systems had been utilized for targeting the LS.[5]

Amongst the lipid-based nanocarriers, solid lipid nanoparticles (SLN), are colloidal carriers composed of a solid lipid core surrounded by a surfactant coat as a stabilizing agent.[7] The major components of SLN are solid lipids, which have low toxicity, biocompatibility, and biodegradability.[8] Furthermore, the incorporation of the drug within the lipid core protects it from chemical degradation and controls drug release if desirable.[9] In addition, drug absorption through the intestinal membrane occurs either through the nanoparticle uptake mechanism or through passive drugs transported after dissolution.[10] Besides, the nano-sized and presence of lipid materials enhances LDD through M cells.[4] Interestingly, the decoration of nanocarriers with PEG enhances their intestinal retention and intestinal permeability.[11] Along with this, the conjugation of vitamin E to PEG enhances the permeability of drugs susceptible to efflux transporters.[12] Therefore, lipid-based nanocarriers with desirable physicochemical properties were developed to enhance LDD. Herein, the incorporation of D-α-Tocopherol polyethylene glycol 1000 succinate (TPGS) within the LDD system enhances intestinal retention and inhibits drug efflux toward the intestinal lumen after absorption by enterocytes.[13]

Gefitinib (GEF), a lipophilic drug, is a member of tyrosine kinase inhibitors that prevents auto-phosphorylation of epidermal growth factor receptors (EGFRs). EGFRs are commonly overexpressed on the membranes of highly proliferated tumor cells including lung cancer.[9] GEF is approved by the FDA as a first-line for the treatment of non-small cell lung cancer.[14] Furthermore, GEF is documented to inhibit the growth of different cancer cell lines, such as colorectal cancer,[15] breast cancer,[16] and hepatocellular carcinoma.[17] Unfortunately, GEF exhibits low drug bioavailability as a result of its low aqueous solubility, first-pass metabolism, and susceptibility to efflux transporters.[18] Moreover, various side effects including diarrhea, skin rash, and left ventricular dysfunction have been observed as a result of a wide distribution of GEF to normal cells.[9,19] Therefore, enhancing the GEF dissolution rate increases the therapeutic index, which in turn decreases the administered dose. In addition, targeting the LS using the LDD system ensures the elimination of metastatic cancer cells and prevents cancer relapse.[5]

The present study aimed to develop GEF-loaded solid lipid nanoparticles and GEF-loaded PEGylated solid lipid nanoparticles (GEF-SLN and GEF-P-SLN, respectively) to enhance dissolution, intestinal permeability, lymphatic delivery, and cytotoxicity of GEF. Optimization of SLN and P-SLN was performed based on particle size (PS), zeta potential (ZP), polydispersity index (PDI), and stability. Optimized SLN and P-SLN were loaded with GEF and characterized in terms of in-vitro release and ex-vivo permeability using the rabbit intestine. Cytotoxicity of prepared formulations against the A549 cell line as a surrogate model for lung cancer was studied using an MTT assay. Finally, an

apoptotic study was performed to evaluate and compare the efficiency of free GEF and GEF-P-SLN on the cell death stages.

Materials and Methods

Materials

Gefitinib was purchased from Beijing Mesochem Technology Co. Ltd. (Beijing, China). Pluronic-F68 (PF-68, HLB: 29) and D-α-Tocopherol polyethylene glycol 1000 succinate (TPGS) were purchased from Sigma Aldrich, St. Louis, MO, USA. Tween-80 (T-80, HLB: 15) was purchased from Loba Chemie (Mumbai, India). Stearic acid (SA, long-chain fatty acid) and Tween-20 (T-20, HLB: 16.7) were purchased from BDH (Poole, UK). Kolliwax-GMS (K-GMS, which contains mainly mono-glyceride) was donated by BASF (Ludwigshafen, Germany). Compritol −888 (C-888, mainly di-glyceride) was purchased from Sigma Chemicals Co. (St. Louis, Missouri).

Solubility Study

GEF solubility in different types of solid lipids was studied visually as previously described by Bhalekar et al. One hundred mg of each solid lipid and 10 mg of GEF were mixed in a cylindrical vial and heated up to 80°C. Once the drug dissolved, a further amount of GEF was added until drug precipitation. On the other hand, if 10 mg failed to dissolve, a further amount of solid lipid was added till the formation of a clear solution.[20]

Regarding surfactant, GEF solubility within surfactant was measured as previously described by Patel and Patel.[21] An excess amount of GEF was dispersed in 0.5% surfactant solution in a cylindrical beaker. The obtained mixture was mixed using a magnetic stirrer at 1200 rpm for 72 hrs. The mixture was centrifuged at 10,000 rpm for 10 mins using a Benchtop centrifuge (PrO-Research K2015, Centurion Scientific Ltd., Chichester, UK) and drug concentration was measured using the developed UPLC method.

Preparation of SLN and P-SLN

SLNs formulations were prepared as previously described by Harisa and Badran[22] using the ultrasonic melt-emulsification method with slight modification. Each formulation was prepared as described in Tables 1 and 2. Briefly, an aqueous phase was prepared by mixing the predetermined amount of surfactant and TPGS (in the case of P-SLN) in distilled water. The lipid phase was prepared by adding a weighted amount of solid lipids without (Plain-SLN or Plain-P-SLN) or with GEF (GEF-SLN or GEF-P-SLN) in a cylindrical beaker. During preparation, both beakers are heated up to 80°C simultaneously. The beaker containing liquefied lipid was placed above a preheated Magnetic-Stirrer heater at 80°C and then the hot aqueous phase was added gradually. When the magnetic stir was added, the mixing speed was increased by up to 5000 rpm for 3–5 minutes to obtain the primary microemulsion. After that, SLN was obtained from primary hot microemulsion using probe-sonication (Bandelin Sonopuls HD 220, Bandelin Electronic, Germany) at 80% voltage efficiency for 3 min; each cycle was 10 seconds followed by 5 second resting period. The obtained SLN was placed immediately in the refrigerator until cooling.

Optimization of Formulation Factors

Effect of Solid Lipid Type and Concentration

Three Plain-$SLN_{1\text{-}3}$ formulations consisting of different solid lipids (C-888 or K-GMS or SA, respectively) and PF-68 were prepared to study the effect of lipid type on the physicochemical properties of SLN. Additionally, Plain-$SNLN_{3\text{-}6}$ formulations containing different SA concentrations and PF-68 were prepared to study the effect of lipid concentration on the physicochemical properties of SLN.

Effect of Surfactant Type and Concentration

Plain-$SLN_{5,7 \text{ and } 8}$ formulations containing different types of surfactants (PF-68 or T-20 or T-80, respectively) and SA were prepared to select the best surfactant based on the physicochemical properties. Further, Plain-$SLN_{5 \text{ and } 9\text{–}11}$ formulations containing different PF-68 concentrations and SA were prepared to study the effect of surfactant concentration on the physicochemical properties of SLN.

Table 1 Composition of the Prepared Plain-SLN

Formulation Code	Solid Lipid (mg)			Surfactant (mg)			
	C-888	K-GMS	SA	PF-68	T-20	T-80	TPGS
Plain-SLN_1	600			100			
Plain-SLN_2		600		100			
Plain-SLN_3			600	100			
Plain-SLN_4			800	100			
Plain-SLN_5			1000	100			
Plain-SLN_6			1200	100			
Plain-SLN_7			1000		100		
Plain-SLN_8			1000			100	
Plain-SLN_9			1000	200			
Plain-SLN_{10}			1000	500			
Plain-SLN_{11}			1000	1000			
Plain-P-SLN			1000	200			20

Notes: The amount was expressed in mg unit. In all formulations, the predetermined amount of surfactant was dissolved in 20 g distilled water as a continuous phase.
Abbreviations: Plain-SLN, drug free-solid lipid nanoparticle; Plain-P-SLN, drug-free-PEGylated solid lipid nanoparticle; C-888, Compritol-888; K-GMS, kolliwax glycerol monostearate; SA, stearic acid; PF-68, Pluronic F-68; T-20, tween 20; T-80, tween 80; TPGS, D-α-Tocopherol polyethylene glycol 1000 succinate.

Table 2 Composition of the Prepared GEF-SLN and GEF-P-SLN

Formulation Code	SA	PF-68	TPGS	GEF
GEF-SLN_1	1000	200	0	10
GEF-SLN_2	1000	200	0	20
GEF-SLN_3	1000	200	0	30
GEF-SLN_4	1000	200	0	40
GEF-SLN_5	800	200	0	40
GEF-SLN_6	600	200	0	40
GEF-P-SLN	1000	200	20	40

Notes: The amount was expressed in mg unit. In all formulations, the predetermined amount of surfactant was dissolved in 20 mL distilled water as a continuous phase.
Abbreviations: GEF-P-SLN, gefitinib-loaded PEGylated solid lipid nanoparticle; SA, stearic acid; PF-68, Pluronic F-68; TPGS, D-α-Tocopherol polyethylene glycol 1000 succinate; GEF, gefitinib.

Effect of Solid Lipid/ Drug Ratio

To study the effect of lipid/drug ratio with fixed lipid concentration on the physicochemical properties, GEF-SLN_{1-4} containing 100, 50, 33.33, and 25 solid lipid/drug ratios, respectively, were prepared. Furthermore, GEF-SLN_{4-6} containing lipid/drug ratios (15, 20, and 25, respectively) with fixed drug concentrations were prepared to study the effect of lipid content on the physicochemical properties of SLN in the presence of GEF. Finally, GEF-P-SLN was prepared similar to GEF-SLN_4 except that 20 mg of TPGS was dissolved in aqueous media.

Physicochemical Characterization

Particle Size (PS), Polydispersity Index (PDI), and Zeta Potential (ZP)

PS, PDI, and ZP for each formulation were measured using a Zetasizer Nano ZS [Malvern Instruments, UK]. Each formulation was diluted (1:1000) in distilled water and evaluated at 25°C. Particle size (besides PDI) and ZP were measured using Dynamic Light Scattering (DLS) and Laser Doppler Velocimetry (LDV) modes, respectively. The found values will be taken as an average of three measurements where each value was reported as an average of six measurements.[22]

DSC

SLN_4 and SLN_6 were subjected to DSC analysis using the DSC−8000 Perkins Elmer (Waltham, MA, USA) apparatus in a temperature range of 25–205°C at two different heating rates of 20 and 100°C/min. The samples were evaluated with the purge of nitrogen at around 20 mL/min, and an autosampler and chiller were installed on this apparatus. The weight of each sample was 3 mg and fixed inside the sealed aluminum pan. For the characterization and evaluation of the samples, a Pyris manager software (Pyris Elmer, Waltham, MA, USA) was used for the solid-state characterization.[23]

PXRD

The PXRD spectra of the GEF, SA, freshly melted and cooled SA, PF-68, SLN_4, and SLN_6 were performed to evaluate the molecular state of SA and GEF crystallinity after preparing SLN. The study was conducted using an X-ray diffractometer (Ultima IV, Rigaku Inc. Tokyo, Japan) with a scanning rate of 0.5/min in the scanning range of 3–180°. The characteristic peak of each sample was assessed by collecting the data by monochromatic radiation (Cu Kα′ 1, λ = 1.54 Å), operating at a voltage of 40 kV and a current of 40 mA.[23]

Encapsulation Efficiency [EE %]

The EE% of the GEF in drug-loaded SLN was measured by the indirect method. Briefly, a predetermined amount from the prepared formulation was centrifuged for 30 min at 50,000 rpm to precipitate loaded SLN. The amount of the drug in the supernatant will be measured using the developed UV-UPLC method. EE% will be determined using Equation 1.[24]

$$EE\% = (total\ amount\ of\ GEF\ (mg) - amount\ of\ GEF\ in\ supernatant\ (mg)/total\ amount\ of\ GEF\ (mg) * 100\% \quad (1)$$

In-vitro Dissolution

In-vitro release of GEF was performed using a previously described dialysis method with minor modification.[25] An amount equivalent to a drug suspension or formulation containing 0.5 mg of GEF diluted [1:4] in phosphate buffer was placed inside a dialysis membrane bag (molecular weight cut off: 12–14 kDa) and sealed. This bag was placed in a beaker containing a preheated 100 mL medium of simulated intestinal fluid (pH 6.8) containing 0.5% T-80. The beaker was continuously shaken at 100 rpm at 37±1°C in a thermostat shaker. Samples were withdrawn at 5, 10, 15, 30, 30, 60, 120, 240, 480, 720, 960, and 1440 minutes and an equal amount of dissolution media was replaced. The withdrawn samples will be centrifuged for 10 min at 10,000 rpm and the amount of drugs in the supernatant was determined using the developed UV-UPLC method.

Kinetic release for all formulations was performed to determine drug release patterns and behavior of formulations during the dissolution study. It was determined through appropriate calibration as follows: zero-order (time versus cumulative % drug release), first-order (time versus log % cumulative drug remaining), Higuchi's (square root of time versus cumulative % drug release), and Korsmeyer-Peppas release model (log time versus log % cumulative drug release). The correlation coefficient (r^2) and n value for each formulation were calculated and an appropriate explanation was performed.

Ex-vivo Permeability

Protocol

Ex-vivo permeability was performed using a New Zealand rabbit with a body weight of 2 Kg, it was housed under standard laboratory conditions (12 h:12 h light/dark cycles at 25±2°C) with free access to standard pellet food and water

ad libitum. The rabbit was maintained under normal conditions for 1 week to acclimatize them to the laboratory environment. The rabbit received care in compliance with the guidelines set by the Animal Care and Use Committee of our institute and the National Institutes of Health. The rabbit was sacrificed and the small intestine was instantly excised and kept in a Krebs buffer solution (7 g/L sodium chloride, 0.34 g/L potassium chloride, 46.8 mg/L magnesium chloride, 0.207 g/L sodium dihydrogen phosphate, 0.251 g/L disodium hydrogen phosphate, and 1.8 g/L glucose, pH 6.5). The small intestine was cut into accurately measured segments, and the inner lumen was rinsed with Krebs buffer to get rid of luminal content. One side was tied and an equivalent amount from drug suspension or formulation (containing 2 mg GEF) diluted (1:1) in phosphate buffer was placed inside the intestinal lumen from the other side and tied. The intestinal segment was placed inside a tube containing 10 mL of phosphate buffer (pH 7.4, 0.5% T-80). The temperature was maintained at 37 ± 0.5°C.

Samples Collection and Analysis

At predetermined time intervals (30, 60, 120, 240, 480, and 720 minutes), the sample was taken and replaced equal volume of fresh buffer. The sample was diluted with acetonitrile [3:1] to participate in any biological tissue and centrifuged at 10,000 rpm for 10 minutes. The amount of drugs in the supernatant was determined using the developed UPLC method.

Data Analysis

The accumulative amount of GEF permeated per cm^2 was plotted against time [minutes]. Apparent permeability coefficient (Papp) and permeability enhancement ratio [PER] were calculated from the Equations (2) and (3), respectively.

$$Papp = dQ/(dt * A * C_o) \quad (2)$$

where A is the area of the tissue (cm2), dQ/dt is the steady-state appearance rate on the acceptor side of the tissue and Co is the initial concentration of the drug in the donor compartment.

$$PER = Papp\ of\ the\ SLN\ formulation/Papp\ of\ the\ drug\ suspension \quad (3)$$

Cell Culture

Human non-small-cell lung carcinoma (NSCLC) cell lines (A549) were obtained from DSMZ Leibniz Institute (German Collection of Microorganisms and Cell Cultures Braunschweig, Germany). Cells were maintained in the incubator at 37°C in a humidified incubator with 5% CO_2, in DMEM culture medium, supplemented with 10%v/v FBS (Gibco; USA) and 1%v/v penicillin-streptomycin.

In-vitro Cytotoxicity

The cytotoxic evaluation of the selected formulations against A549 cell lines was performed by MTT assay as previously described by Nasr et al.[26] Briefly, cells were plated at 1×10^5 cells per well in 96-well for 24 h. Thereafter, the cells were treated with different concentrations (2.5–20 µg/mL) of pure GEF (dissolved in DMSO), Plain-SLN_9, and drug-loaded formulations (GEF-SLN_4 and GEF-P-SLN). After 48 h of incubation, 10 µL of MTT solution [5 mg/mL] was added to each well and further incubated in the dark for 4 h at 37°C. Next, the formazan product was solubilized with acidified isopropanol and the absorbance was measured at a wavelength of 570 nm using a microplate reader [Bio-Tek, USA]. The dose–response curves were used to calculate the IC50 (concentration required to inhibit cell growth by 50%). Cell viability was calculated according to Equation 4.

$$Cell\ Viability\ (\%) = (optical\ density\ of\ the\ treated\ sample)/(optical\ density\ of\ the\ untreated\ sample) * 100\% \quad (4)$$

Flow Cytometric Analysis of Cells Apoptosis

Flow cytometric analysis was employed to quantify cell apoptosis using an Annexin-V/FITC/PI staining Kit (Sigma, USA) according to the manufacturer's instructions. In brief, A549 cells were seeded in a 12-well plate at a density of 1×10^5 cells/well, and after overnight incubation, the cells were treated with IC_{50} of pure GEF (3.5 µg/mL), as

well as the equivalent concentration of PLAIN-SLN and GEF-C-CSLN. After 48 h of incubation, treated and untreated cells were collected, washed with cold PBS (1x), and resuspended in 100µL of binding buffer (1x) with FITC Annexin V (5 µL) and PI (5 µL). After 20 min incubation in the dark, 400µL of binding buffer was added and the samples were analyzed by flow cytometry (Cytomics FC 500; Beckman Coulter, Brea, CA, USA).[26]

Stability Study

The formulations were placed within a 20 mL glass vial with a rubbery stopper during the stability study. The stability of the prepared Plain-SLN was evaluated in terms of the physicochemical properties at 4°C after 1 month. Furthermore, GEF-SLN and GEF-P-SLN were evaluated in terms of physicochemical properties and EE at 4°C after 7, 15, 22, and 30 days.

UPLC Method

GEF quantification in all samples was analyzed on Dionex™ ultra-high-performance liquid chromatography (UHPLC) equipped with a Dionex™ automatic sample manager and diode array ultraviolet detector (Thermo Scientific, Bedford, MA, USA). A mobile phase consisted of 60:40 (v/v) water: acetonitrile containing (0.1% trimethylamine) pH adjusted to 6.7 with phosphoric acid was pumped at a flow rate of 0.4 mL/min with a total run time of 3 min. The injection volume was 3 µL and the detection wavelength was 250 nm.

Statistical Analysis

All data analyses were performed using SPSS software, Version 26. The results were compared using a one-way analysis of variance (ANOVA) followed by Hochberg or Tukey's test was used to compare three or more data sets. Data were expressed as mean ± SD and p-value <0.05 was used as criteria.

Results

Solubility of GEF in Solid Lipid and Surfactant

The solubility of GEF in different solid lipids (SA, K-GMS, and C-888) was studied. GEF solubility in stearic acid (SA), Kolliwax-GMS (K-GMS), and Compritol −888 (C-888) were 230.8 −285.7, 62.5 −90.9, and 24.4 −32.3 mg/g, respectively. It has been observed that the solubility of GEF was significantly affected by the type of solid lipid esterification. Maximum solubility was observed in SA which consists of free long-chain fatty acid. Additionally, GEF solubility in different surfactants (PF-68, T-20, and T-80) was 3.45 ± 0.55, 42.83 ± 1.64, and 44.93 ± 2.15 µg/mL, respectively.

Optimization of SLN Components and Their Concentrations on Physicochemical Properties of SLN

Effect of Lipid Type

Table 3 shows the physicochemical properties of Plain-SLN that are produced from different types of solid lipid. Additionally, a strong correlation was observed between the degree of fatty acid esterification and particle size as shown in Figure 1A. It has been found that SA produces the smallest SLN with a narrow PDI, whereas C-888 produces the largest particle size. Besides, the negative value of the surface charge produced was arranged in the following order: C-888 > K-GMS > SA. A stability study revealed that the PS of all SLNs was slightly increased during storage in the refrigerator.

Effect of Lipid Concentration

Regarding lipid concentration, it was found that increasing SA concentration significantly produces larger particles as shown in Table 3. Moreover, Figure 1B shows a strong correlation between the SA concentration and particle size of SLN. All formulations exhibit a high degree of homogeneity (PDI value < 0.3). In addition, increasing solid lipid concentration resulted in an increased negative value of the surface charge. It should be noted that during the production of the Plain-SLN_6, a notable amount of lipid was stuck to the wall of the beaker. Furthermore, a high PDI value was

Table 3 The Effect of Lipid Type and Concentration on the Physicochemical Properties of Plain-SLN on 0 and 30 Days

Duration	0 Day			30 Days		
Characterization	**PS**	**PDI**	**ZP**	**PS**	**PDI**	**ZP**
Plain-SLN_1	303.9 ±10.5	0.273 ± 0.013	−20.1 ± 0.68	321.8 ± 5.5	0.299 ± 0.017	−13.1 ± 1.1
Plain-SLN_2	247.6 ± 6.7	0.245 ± 0.012	−17.7 ± 0.84	258.2 ± 6.0	0.302 ± 0.012	−19.9 ± 3.9
Plain-SLN_3	219.8 ± 1.9	0.068 ± 0.022	−14.0 ± 0.11	274.8 ± 4.5	0.094 ± 0.023	−20.4 ± 0.58
Plain-SLN_4	239.5 ± 6.3	0.092 ± 0.011	−18.0 ± 0.15	266.3 ± 2.0	0.092 ± 0.013	−21.0 ± 0.91
Plain-SLN_5	251.5 ± 2.6	0.139 ± 0.052	−21.6 + 0.55	278.3 ± 5.1	0.098 ± 0.017	−21.6 ± 1.73
Plain-SLN_6	264.9 ± 7.2	0.171 ± 0.015	−18.8 ± 0.83	292.6 ± 2.4	0.135 ± 0.025	−21.7 ± 0.66

Note: Data were expressed as the mean ± SD, N = 3.
Abbreviations: Plain-SLN, drug free-solid lipid nanoparticle; PS, particle size; PDI, polydispersity index; ZP, zeta potential.

observed with Plain-SLN_6. During storage, the PS of formulations prepared from the different concentrations of lipid was slightly increased.

Effect of Surfactant Type

Surfactants act as a stabilizer that controls physicochemical properties of SLN, such as PS, PDI, and ZP during the production process.[27] Based on the literature, different surfactants with variable HLB values were selected. Figure 2A shows a strong correlation between the HLB value of the used surfactants and the particle size of SLN. It has been found that decreasing HLB values (29, 16.5, and 15) of the used surfactant resulted in increased particle size (251.5, 291.9, and 307.6 nm) of the prepared Plain-$SLN_{5,\ 7,\ and\ 8}$, respectively. Table 4 shows that PF-68 was able to produce the smallest particle size (251.5 ± 2.6 nm) with a narrow PDI (0.139 ± 0.052) compared to other surfactants. Additionally, T-20 was able to produce a higher negative value on the surface of SLN. It has been found that PF-68 and T-80 were able to stabilize the produced SLN when compared with the T-20.

Effect of Surfactant Concentration

Regarding surfactant concentration, it has been found that increasing the concentration of surfactant produces SLN with a small particle size as shown in Table 4. Also, Figure 2B shows a good correlation between surfactant concentration and the produced particle size. An inversely strong linear correlation has been observed between the used aqueous surfactant

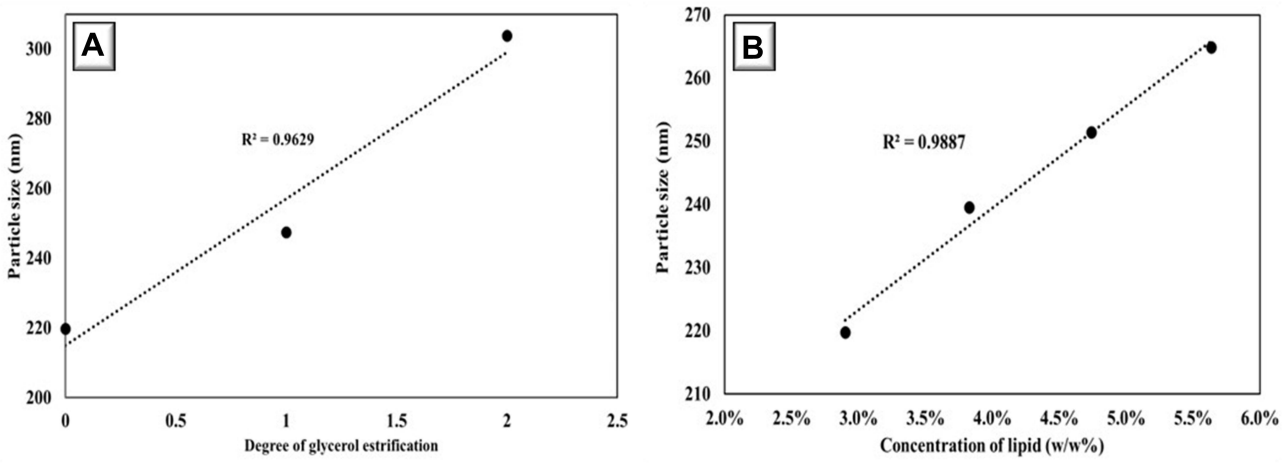

Figure 1 Correlation between (**A**) degree of solid lipid esterification and PS of SLN, and (**B**) solid lipid content and PS of SLN.

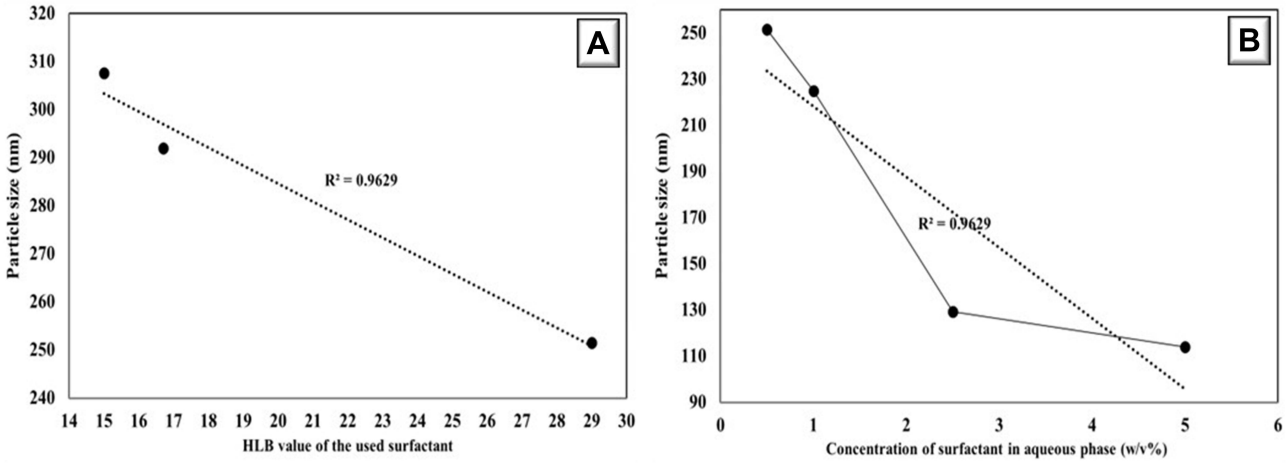

Figure 2 Correlation between (**A**) HLB value of different surfactants and particle size of SLN, and (**B**) surfactant concentration and PS of SLN.

concentration (0.5–2.5%) and PS. Further increase in the surfactant concentration by up to 5% produces a slight reduction in PS. The results revealed that Plain-SLN_9 showed a higher degree of homogeneity when compared with the other concentrations. Moreover, increasing surfactant concentration did not affect the surface charge of the prepared SLN. Plain-SLN_9 was able to stabilize the produced SLN when compared with other concentrations (0.5%, 2.5%, and 5%).

Effect of Solid Lipid/Drug Ratio

It has been observed that decreasing the solid lipid/drug ratio while fixing the amount of solid lipid used resulted in increased particle size of the prepared SLN. Moreover, Figure 3A shows a good reversible correlation between solid lipid/drug ratio and particle size of SLN. On the other hand, Table 5 shows that decreasing the solid lipid/drug ratio while fixing the amount of drug used resulted in increased particle size of the prepared SLN. Furthermore, the reversible correlation between lipid content in the presence of the drug and the obtained particle size of SLN is shown in Figure 3B. Finally, GEF-P-SLN was obtained during the production of SLN from an aqueous phase containing TPGS in addition to PF-68. The PS of GEF-P-SLN was lower when compared with the un-PEGylated GEF-SLN_4.

Table 4 The Effect of Surfactant Type and Concentration on the Physicochemical Properties of Plain-SLN

Duration	**0 Day**			**30 Day**		
Characterization	**PS**	**PDI**	**ZP**	**PS**	**PDI**	**ZP**
Plain-SLN_7	291.9 ± 1.8	0.229 ± 0.017	−27.6 + 0.53	390.2 + 3.56	0.362 + 0.011	−26.6 + 1.76
Plain-SLN_8	307.6 ± 2.2	0.163 ± 0.078	−23.7 + 1.55	336.3 +12.3	0.184 + 0.006	−22.1 + 2.57
Plain-SLN_5	251.5 ± 2.6	0.139 ± 0.052	−21.6 + 0.55	278.3 ± 5.1	0.098 ± 0.017	−21.6 ± 1.73
Plain-SLN_9	224.9 ± 4.3	0.066 ± 0.017	−23.1 + 2.14	239.2 + 3.19	0.078 ± 0.051	−26.7 + 1.41
Plain-SLN_{10}	129.3 ± 2.5	0.147 ± 0.034	−22.3 + 0.67	Particles aggregation was observed		
Plain-SLN_{11}	114.0 ± 4.3	0.350 ± 0.061	−23.5 + 2.35			
Plain-P-SLN	309.6 ± 8.7	0.172 ± 0.018	−22.3 ± 0.64	426.5 ± 9.8	0.224 ± 0.013	−23.2 ± 2.52

Note: Data were expressed as the mean ± SD, N = 3.
Abbreviations: Plain-SLN, drug free-solid lipid nanoparticle; PS, particle size; PDI, polydispersity index; ZP, zeta potential.

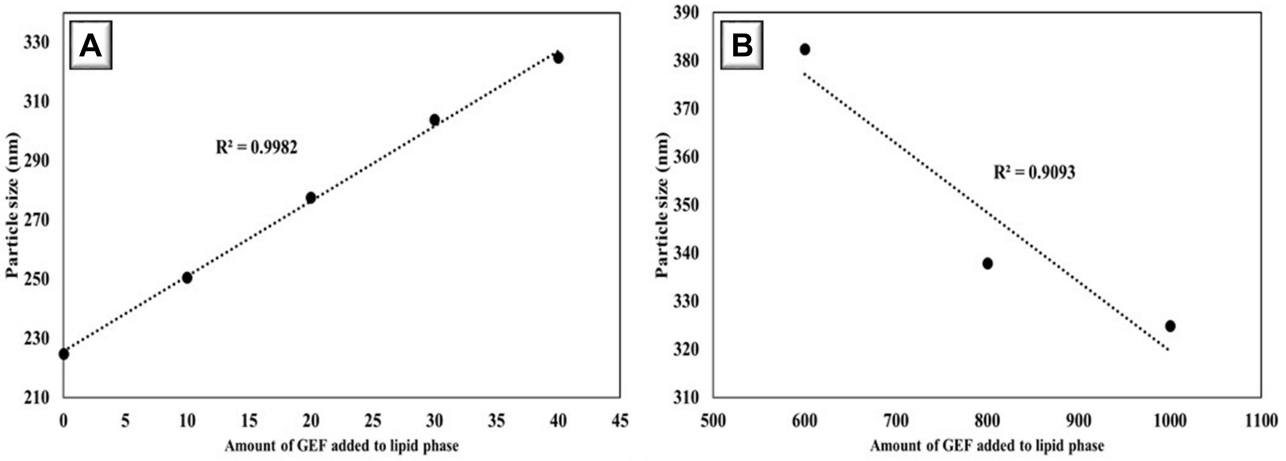

Figure 3 The correlation between solid lipid/ drug ratio and particle size of SLN (**A**) at the same lipid level and (**B**) at the same drug level.

DSC

DSC of pure GEF was previously performed in our lab, and it was melted at 198°C with a characteristic sharp endothermic peak.[23] To observe any degree of GEF crystallinity, GEF-SLN_4, and SLN_6 were subjected to thermal scanning at two different heating rates (20, and 100°C/min). Figure 4 shows that there is no endothermic peak observed for GEF with both formulations even with a faster heating rate (100°C/min). Both formulations exhibited melting peaks at 71°C at a slower heating rate, while they were increased to 85 and 82°C, for GEF-SLN_4, and GEF-SLN_6, respectively, at a faster heating rate.

PXRD

Figure 5 shows the diffraction patterns of raw GEF, raw SA, freshly melted then cooled SA, PF-68, GEF-SLN_4, and GEF-SLN_6. The pure GEF showed multiple peaks with high intensity at 38.1° and 44.3° besides moderate-intensity peaks at 19.4°, 24.2°, 26.4°, and 77.5°. The crystallinity of SA was measured for raw SA and freshly melted then cooled SA to observe the effect of the SLN preparation method on the arrangement of particles. Both SA showed sharp high-intensity diffraction peaks at 21.7° 24.3°, and 38.1°. However, the freshly cooled SA showed additional peaks at 6.7°, 11.1°, and 44.3°. Additionally, PF-68 showed two predominant characteristics peaks at 19.4°, and 23.5°. Finally, both GEF-SLN_4 and GEF-SLN_6 showed their characteristic diffraction peaks at 6.7°, 21.6°, and 24.2,° while the intensity was lower in the GEF-SLN_6.

Table 5 the Effect of Drug Loading and Lipid Content on the Physicochemical Properties of GEF-SLN

Characterization	PS	PDI	ZP	EE %
GEF-SLN_1	250.7 ± 5.4	0.112 ± 0.042	−22.9 ± 1.00	91.32 ± 1.7
GEF-SLN_2	277.6 ± 3.0	0.138 ± 0.038	−19.5 ± 2.90	92.38 ± 3.5
GEF-SLN_3	303.9 ± 8.4	0.169 ± 0.033	−21.7 ± 0.60	90.45 ± 2.0
GEF-SLN_4	324.9 ± 4.0	0.139 ± 0.051	−21.0 ± 0.90	91.17 ± 2.8
GEF-SLN_5	338.0 ± 2.7	0.172 ± 0.009	−24.0 ± 1.06	89.40 ± 1.9
GEF-SLN_6	382.5 ± 6.4	0.216 ± 0.009	−24.1 ± 1.32	90.58 ± 1.7
GEF-P-SLN	286.8 ± 11.8	0.124 ± 0.008	−22.3 ± 1.00	91.25 ± 2.1

Note: Data were expressed as the mean ± SD, N = 3.
Abbreviations: GEF-SLN, gefitinib-loaded solid lipid nanoparticle; GEF-P-SLN, gefitinib-loaded PEGylated solid lipid nanoparticle; PS, particle size; PDI, polydispersity index; ZP, zeta potential.

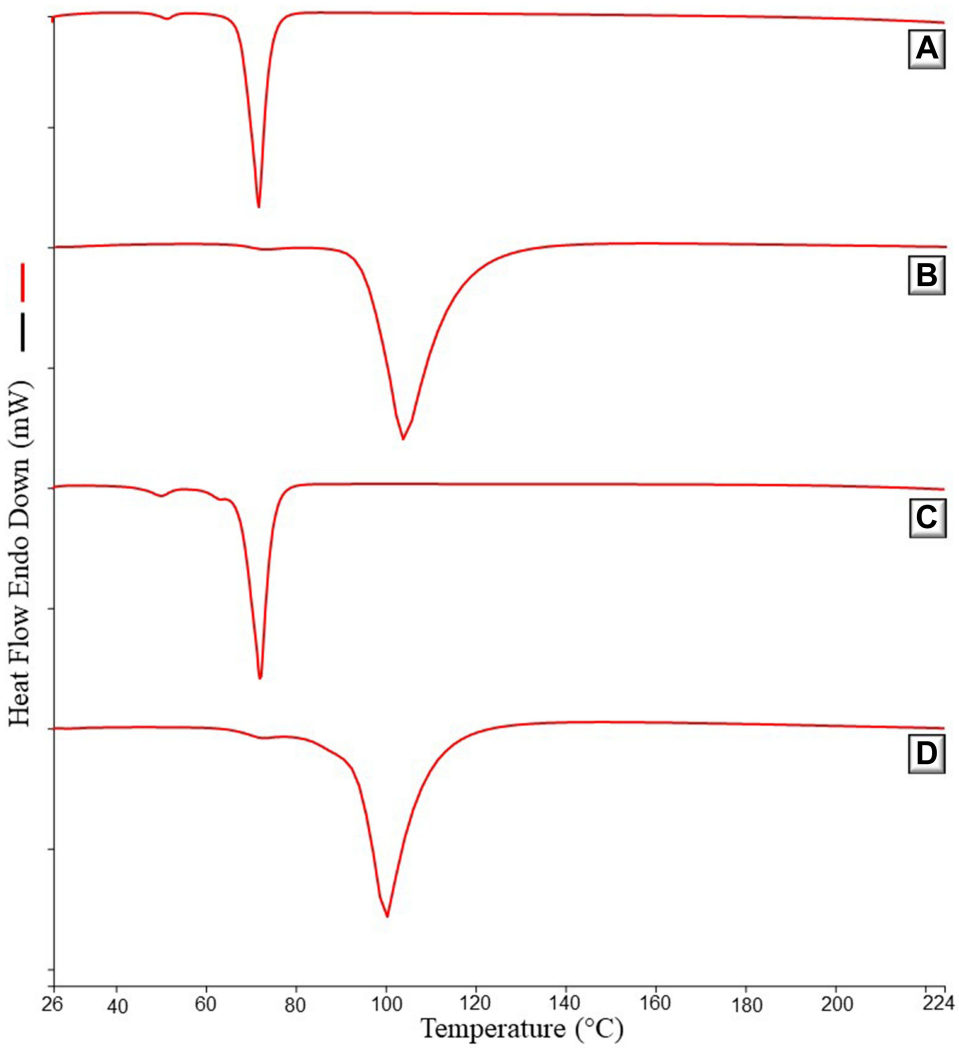

Figure 4 DSC of GEF-SLN$_4$ heated at rate (**A**) 20°C/min, and (**B**) 100°C/min, and GEF-SLN$_6$ heated at rate (**C**) 20°C/min, and (**D**) 100°C/min.

Figure 6 shows beakers containing A) SA, B) physical mixture of SA: GEF (25:1), and C) physical mixture of SA: GEF (15:1) were melted and mixed until obtaining a clear solution of SA then cooled. The second and third mixtures resemble high and low solid lipid/drug ratios that are used to prepare SLN$_4$ and SLN$_6$, respectively. The incorporation of GEF in melted SA resulted in a different morphological crystalline appearance when compared with pure SA. Moreover, the obtained lipid was crushed and scanned with SEM to observe the surface morphology of crystals. The surface of the obtained crystals was smooth in the case of pure SA, while it was rough in the case of SA: GEF mixtures as shown in Figure 6D–F.

SEM

Electronic imaging of Plain-SLN GEF-SLN, Plain-P-SLN, and GEF-P-SLN are shown in Figure 7A–D, respectively. It is clear from the image that the particles are slightly aggregated. However, Un-PEGylated SLN either unloaded or loaded with GEF is well separated when compared with PEGylated SLN. It was observed that Plain-SLN is spherical and regular in shape when compared with oval and irregular particles of GEF-SLN. This agrees with the visual observation shown in Figure 7E. Plain-SLN and GEF-SLN were placed in Eppendorf and flipped to observe sickness of formulation to the wall. It was found that Plain-SLN is free-flowing after flipping, while GEF-SLN is sticky to the surface of Eppendorf. Figure 7C and D show that Plain-P-SLN and GEF-P-SLN are sticky to each other.

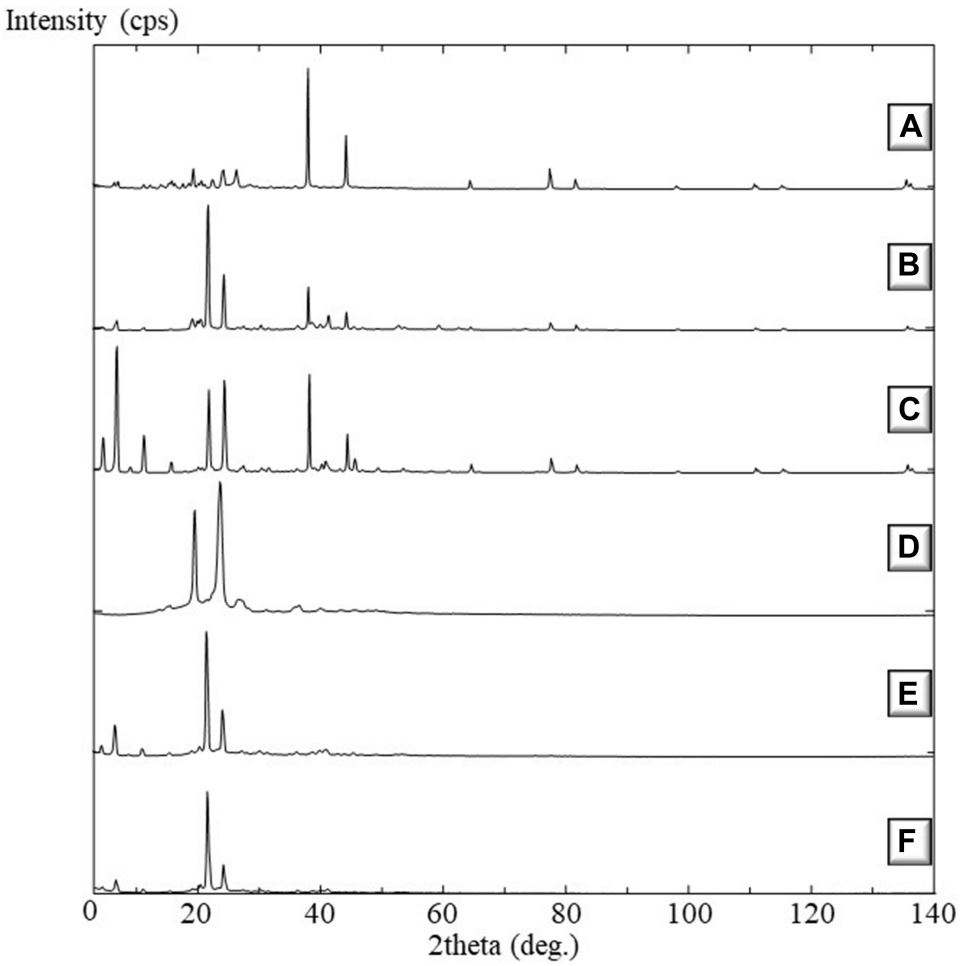

Figure 5 PXRD of (**A**) GEF, (**B**) SA, (**C**) freshly melted and cooled SA, (**D**) PF-68, (**F**) SLN_4, and (**E**) SLN_6.

In-vitro Release

Figure 8A and B shows the initial and cumulative percent of GEF released, respectively, from pure GEF, GEF-$SLN_{4\text{-}6,}$ and GEF-P-SLN. Kinetics analysis of the drug release was performed for all formulations to evaluate the behavior of SLN during the dissolution study as shown in Table 6. It has been found that the drug release pattern for all formulations was different in the initial (first 1 hr) and final stage (2–24 hrs). Therefore, the kinetics analysis was performed two times for each formulation (initial; 0–1 hr, and overall; 0 −24 hrs, release profile). Kinetic analysis of the initial stage in the first hour for all formulations mostly exhibited zero-order drug release. However, drug release patterns during the overall stage for the formulations were following the Higuchi model. Finally, GEF-SLN_4 and GEF-P-SLN exhibited faster drug release when compared with the other formulations.

Ex-vivo Permeability

Figure 9A shows the cumulative amount of GEF permeated per unit area (μg/cm^2) at the predetermined intervals. It was found that GEF exhibited initial slow drug permeability in all tested formulations. In particular, the total amount of GEF permeated per unit surface area during the experiment was 4.5, 7, and 11 μg/cm^2 from GEF suspension, GEF-SLN, and GEF-P-SLN, respectively. It was found that GEF permeability across the intestinal membrane was time-dependent. Significant enhancement in drug permeability from the prepared formulation by the time compared to a drug suspension.

The apparent permeability coefficient (Papp) is usually used to express the overall rate of drug flux through the biological membrane during the period of the experiment. The Papp for the GEF suspension, GEF-SLN, and GEF-P-SLN

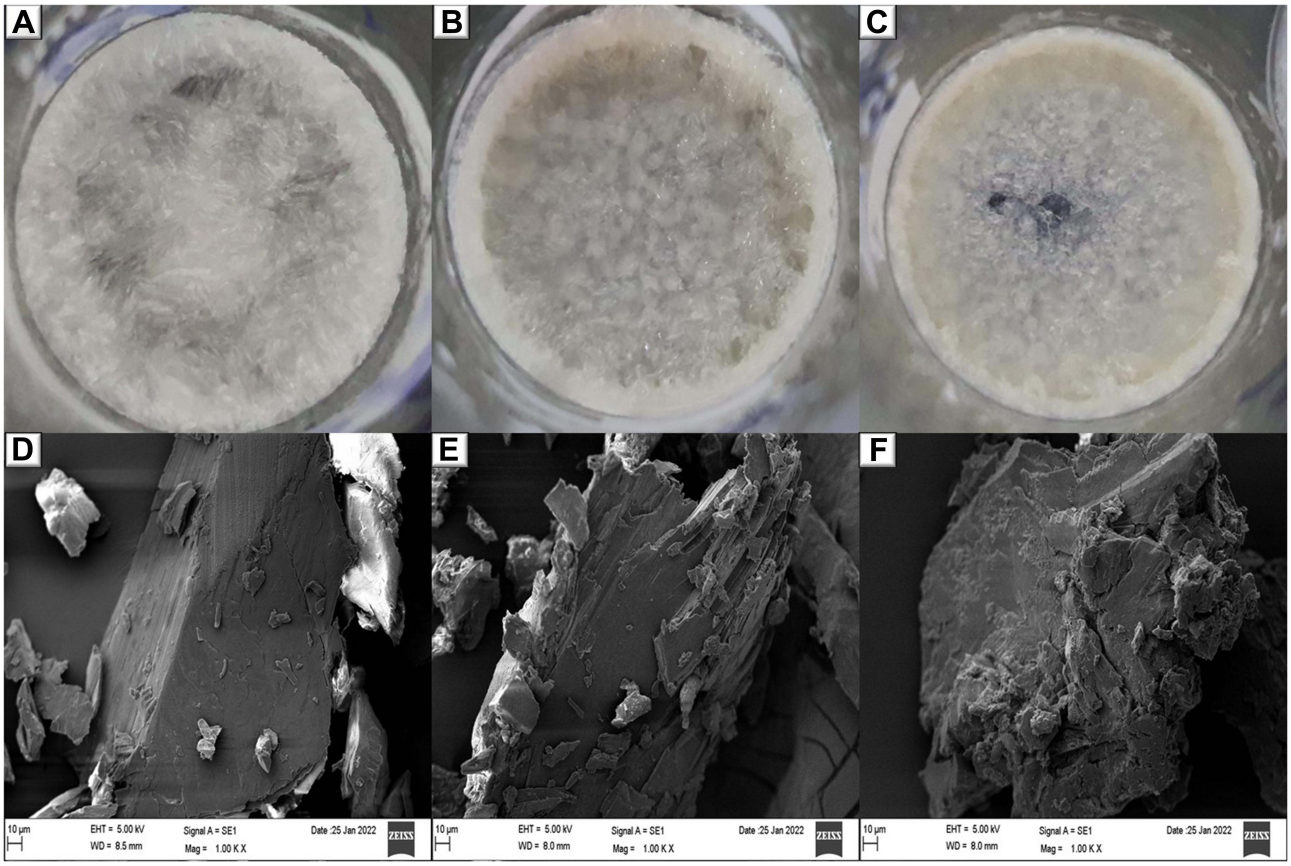

Figure 6 Morphological appearance and SEM image of crushed crystal of (**A** and **D**) SA, (**B** and **E**) physical mixture of SA: GEF (25:1), (**C** and **F**) physical mixture of SA: GEF (15: 1). The agents were physically mixed and heated to obtain GEF dissolved in liquified SA and then cooled in the refrigerator.

is 1.66×10^{-4}, 2.85×10^{-4}, and 4.39×10^{-4} µg/cm^2/hr, respectively. It has been found that all prepared formulations (GEF-SLN and GEF-P-SLN) were able to enhance GEF permeability through the intestinal membrane significantly ($p < 0.05$ and < 0.001, respectively) when compared with GEF suspension. Also, the permeability enhancement ratio gives a numerical value of the effect of the formulation on the drug permeability when compared with a pure drug suspension. It has been found that GEF-SLN and GEF-P-SLN were able to significantly enhance the permeability of GEF by 1.71 and 2.64, respectively, as shown in Figure 9B.

In-vitro Cytotoxicity

The inhibitory effects of pure GEF (dissolved in DMSO), Plain-SLN, GEF-SLN, and GEF-P-SLN on the growth of A549 cells were studied using an MTT assay. Figure 10 shows the cell viability at four different concentrations (2.5, 5, 10, and 20 µg/mL) of pure GEF, Plain-SLN, GEF-SLN, and GEF-P-SLN. It should be noted that equivalent volume from Plain-SLN was added to the cells like a drug-loaded formulation. All formulations inhibited the growth of A549 cells in a concentration-dependent manner. Among all tested formulations, GEF-P-SLN exerted the highest inhibitory level at the lower concentrations (2.5 and 5 µg/mL). Moreover, pure GEF exerted lower cell death activity compared to GEF-SLN, and GEF-P-SLN at 2.5, 5, and 10 µg/mL concentrations. However, pure GEF exerted similar cell death activity (approximately 85%) to GEF-SLN and GEF-P-SLN at 20 µg/mL concentration. Furthermore, GEF-P-SLN enhanced cell death at 2.5 and 5 µg/mL concentrations when compared with GEF-SLN. However, there is no significant difference in enhancement in cell death occurred at 10 and 20 µg/mL concentrations for GEF-SLN and GEF-P-SLN. In addition, Table 7 shows that IC_{50} for Plain-SLN, Pure GEF, GEF-SLN, and GEF-P-SLN was 8.46, 3.5, 1.95, 1.8 µg/mL, respectively. It was found that GEF-SLN and GEF-P-SLN decrease IC_{50} of pure GEF by 1.79 and 1.94-fold, respectively.

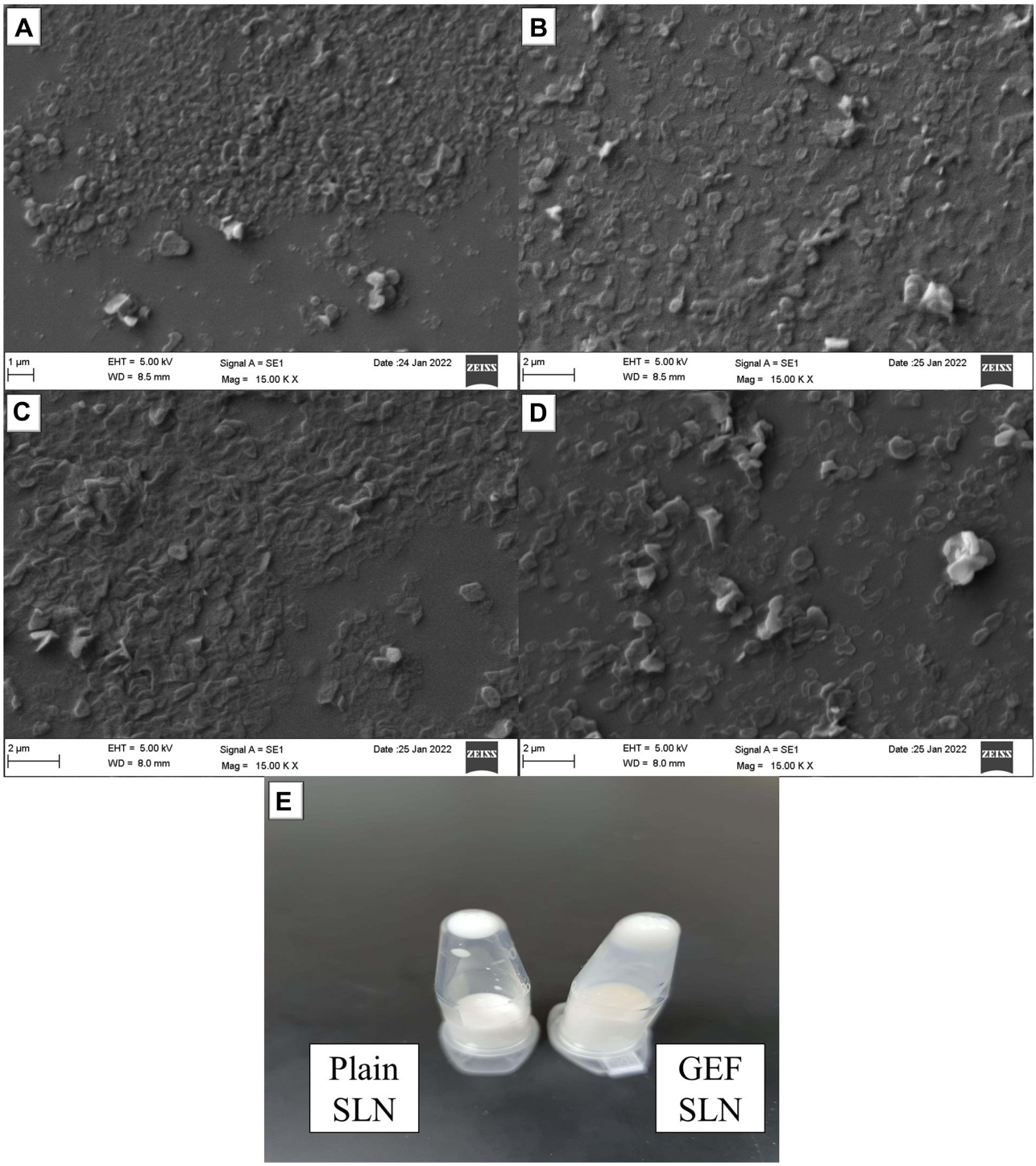

Figure 7 Indicates SEM images of (**A**) Plain-SLN, (**B**) GEF-SLN, (**C**) Plain-P-SLN and (**D**) GEF-P-SLN. (**E**) shows the morphology of Plain-SLN (left), and GEF-SLN (right) after being placed in Eppendorf and flipped to visualize adherence of SLN to the surface.

Apoptosis Study

In the present study, Annexin V/PI double staining was utilized to stain A549 cells following their treatment with Plain-SLN, pure GEF, and GEF-P-SLN for 48 hrs. The cells were treated with 3.5 µg/mL from all formulations which are equivalent to IC_{50} of pure GEF. This concentration was selected based on an MTT assay to observe the augmentation effect produced by GEF-P-SLN when compared with pure GEF. As shown in Figure 11, pure GEF

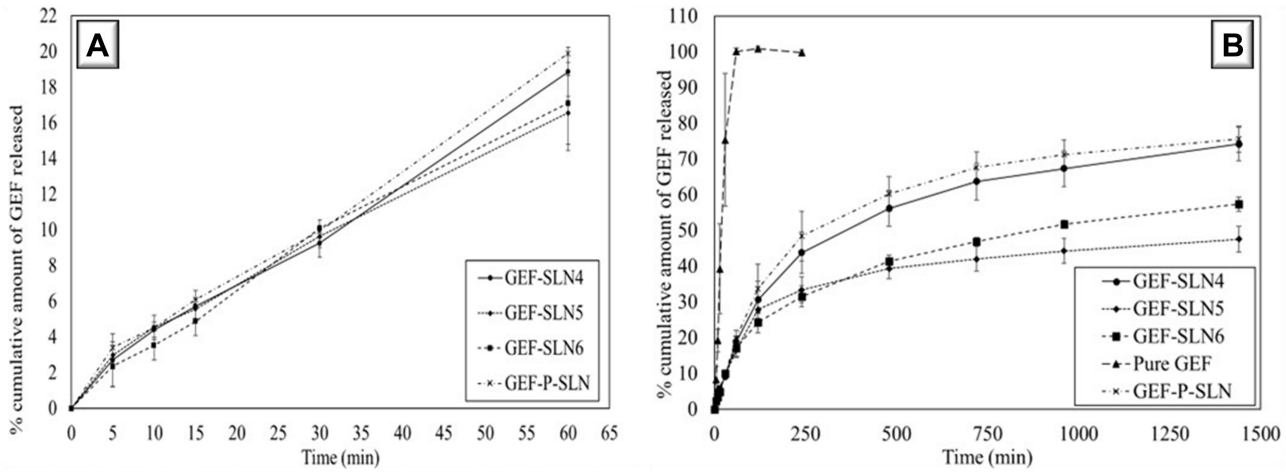

Figure 8 (**A**) Initial and (**B**) Cumulative in-vitro drug release profile from GEF-SLN4-6 and GEF-P-SLN in phosphate buffer containing 0.5% T-80.
Note: Data were expressed as the mean ± SD, N = 3.
Abbreviations: GEF-SLN, gefitinib-loaded solid lipid nanoparticle; GEF-P-SLN, gefitinib-loaded PEGylated solid lipid nanoparticle.

exposure at 3.5 µg/mL concentration led to an increase in both early and late apoptotic cells population (42.47 ± 5.35 and 5.97 ± 1.07%, respectively) compared to untreated cells (2.37 ± 0.06 and 1.87 ± 0.06, respectively). Interestingly, we noticed a significant enhancement of both early and late apoptotic cells population (increased int 83.77 ± 1.70 and 11.87 ± 4.43% respectively) after cells treatment with GEF-P-SLN at the same concentration.

Stability Study

The stability of GEF-SLN and GEF-P-SLN was evaluated in terms of physicochemical characterization and EE every 7–8 days for 1 month as shown in Table 8. The particle size of the prepared formulations was increased for both formulations during storage while keeping a negative surface charge. It was observed that EE of GEF decreased over time during storage.

Table 6 Kinetic Analysis of in-vitro Drug Release During Initial and Overall Stage for GEF-SLN$_{4\text{-}6}$ and GEF-P-SLN

Stage		**Initial Release**				**Overall Release**			
Formulation		**GEF-SLN4**	**GEF-SLN5**	**GEF-SLN6**	**GEF-P-SLN**	**GEF-SLN4**	**GEF-SLN5**	**GEF-SLN6**	**GEF-P-SLN**
r	Zero	0.997	0.999	0.998	0.998	0.913	0.852	0.902	0.885
	First	−0.998	−1.000	−0.997	−0.997	−0.950	−0.884	−0.956	−0.942
	Higuchi	0.992	0.992	0.981	0.978	0.983	0.949	0.978	0.969
	Higuchi Confirm	0.995	0.997	0.995	0.987	0.982	0.975	0.986	0.984
Slope	Zero	0.273	0.246	0.289	0.301	0.039	0.031	0.052	0.054
	First	−0.001	−0.001	−0.001	−0.001	0.000	0.000	0.000	0.000
	Higuchi	2.779	2.496	2.910	3.020	1.615	1.329	2.177	2.258
	Higuchi Confirm	0.825	0.692	0.766	0.714	0.572	0.507	0.609	0.595

Abbreviations: GEF-SLN, gefitinib-loaded solid lipid nanoparticle; GEF-P-SLN, gefitinib-loaded PEGylated solid lipid nanoparticle.

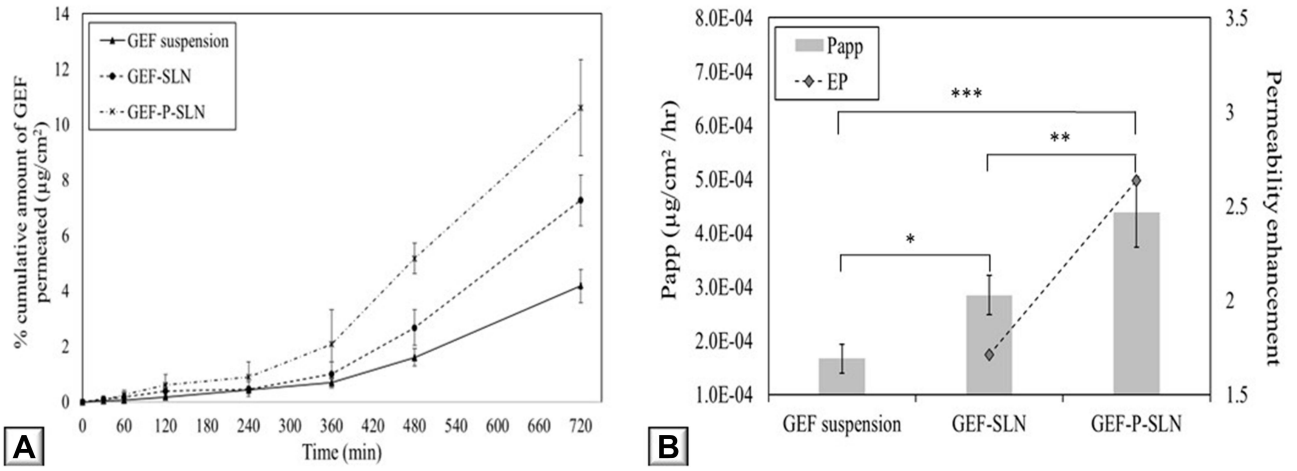

Figure 9 (**A**) Cumulative amount of GEF permeated through the intestinal membrane of rabbit, and (**B**) apparent permeability coefficient (Papp) and permeability enhancement ratio for GEF suspension, GEF-SLN, and GEF-P-SLN.
Notes: Data were expressed as the mean ± SD, N = 3, p-value significant at *0.05, **0.01, and ***0.001.
Abbreviations: GEF-SLN, gefitinib-loaded solid lipid nanoparticle; GEF-P-SLN, gefitinib-loaded PEGylated solid lipid nanoparticle.

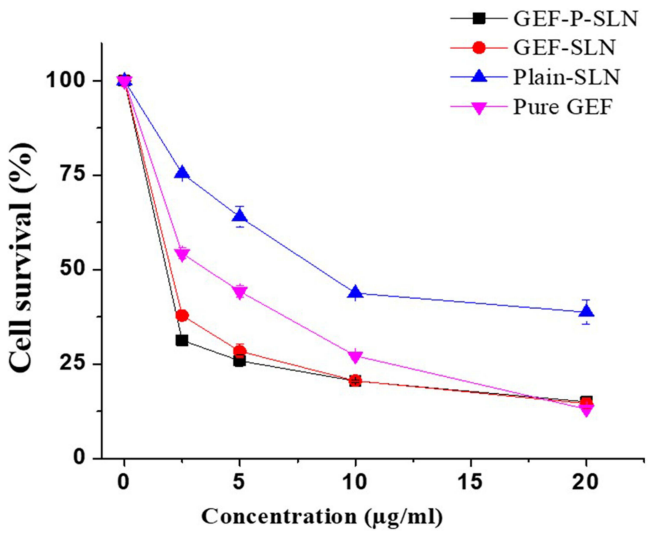

Figure 10 Effect of pure GEF, Plain-SLN, GEF-SLN, and GEF-P-SLN on cell viability of A549 cell line using MTT assay treated with different concentrations (2.5, 5, 10, and 20 µg/mL) after 48 h.
Note: Data were expressed as the mean ± SD, N = 3.
Abbreviations: Plain-SLN, drug-free solid lipid nanoparticle; GEF-SLN, gefitinib-loaded solid lipid nanoparticle; GEF-P-SLN, gefitinib-loaded PEGylated solid lipid nanoparticle.

Discussion

The selected solid lipids during this study consisted of long-chain fatty acids (LC-FAs) rather than medium or short-chain FA. This enhances bile salts sections, which facilitate the formation of colloidal particles within the intestine lumen.[9] Likewise, LC-FAs increase lymphatic drug delivery as a result of increased hydrophobicity of absorbed lipids. This is attributed to the normal absorption pathway of LC-FAs where they are usually transported through the lymphatic system.[21] Therefore, the administered drugs are assembled within chylomicron during their production inside enterocytes.[5]

Table 7 IC50 for All Formulations on the A549 Cells Using MTT Assay

Sample	IC50 (µg/mL)
Pure drug	3.50
GEF-SLN	1.99
GEF-P-SLN	1.83
Plain-P-SLN	8.49

Abbreviations: Plain-SLN, drug-free solid lipid nanoparticle; GEF-SLN, gefitinib-loaded solid lipid nanoparticle; GEF-P-SLN, gefitinib-loaded PEGylated solid lipid nanoparticle.

Solubility of GEF in Solid Lipid and Surfactant

Maximum solubility was observed in SA as a result of the acidic microenvironment produced by the free carboxylic group. This enhances ionization and the solubility of weak basic GEF.[9] Furthermore, a low drug solubility was observed in C-888 when compared with K-GMS. This could be attributed to the abundance of GMS in K-GMS, which was reported to have an intrinsic self-emulsifying effect.[21] In agreement with the obtained results, Dhairyasheel et al studied the solubility of GEF in different liquid oils. It was found that GEF exhibited the highest solubility in oleic acid (LC-FA) when compared with olive and castor oil (LC-triglycerides.[28] In contrast, Nayek et al found that GEF exhibited much higher solubility in phospholipid (LC-DG) than GMS (LC-MG), while LC-FA was not involved in the study. This could be attributed to the use of different solubility evaluation methods. The reported method involved using DMSO in solubility determination which could affect the accuracy of the method.[9]

For the used surfactant, lower drug solubility in surfactant is required to avoid drug deposition on the surface of SLN which causes burst drug release once it exposes to aqueous media.[21] It has been found that GEF exhibited minimum solubility in PF-68 when compared with T-20 and T-80. It should be noted the selection of surfactants is not solely dependent on drug solubility. The effect of surfactant as a stabilizer on physicochemical properties and stability should be considered during its selection.

Optimization of SLN Components and Their Concentrations on Physicochemical Properties of SLN

Optimum formulation during each stage was selected based on the LDD goal as follows. It has been found that nanoparticles are highly susceptible to intestinal transport through enterocytes or M cells.[27,29] Furthermore, SLN with neutral or negative surface charges is more susceptible to lymphatic uptake through M cells.[27] Finally, therefore, SLNs with the smallest particles and highly negatively charged are highly susceptible to lymphatic delivery.

Effect of Lipid Type

In alignment with the obtained results, Khalil et al found that SLN produced by GMS was smaller than the one produced from C-888 at the four different levels of PF-68 concentrations (0.5, 1, 2.5, and 5%). The authors refer to the higher viscosity of C-888 which decreases the effective force applied and transmitted during the production process.[30] Furthermore, Öztürk et al found that the PS of the prepared SLN was arranged in the descending order as follows: tripalmitin (LC-TG) > Glyceryl behenate (LC-MG) > stearic acid (LC-FA). The author refers this to as the reduction in the molecular weight of the used solid lipid.[31] On the contrary, Zardini et al noticed that an increased degree of glycerol esterification resulted in decreased PS. The author referred to this as decreasing melting point of solid lipid which is confirmed by DSC.[29]

Amongst the used solid lipids, SA was selected as the optimum solid lipid component. This is attributed to its solubilization efficiency when compared with other solid lipids. Higher drug solubility of the drug in the solid lipid is required to achieve maximum entrapment efficiency.[32] Additionally, SA was able to produce SLN with the smallest PS

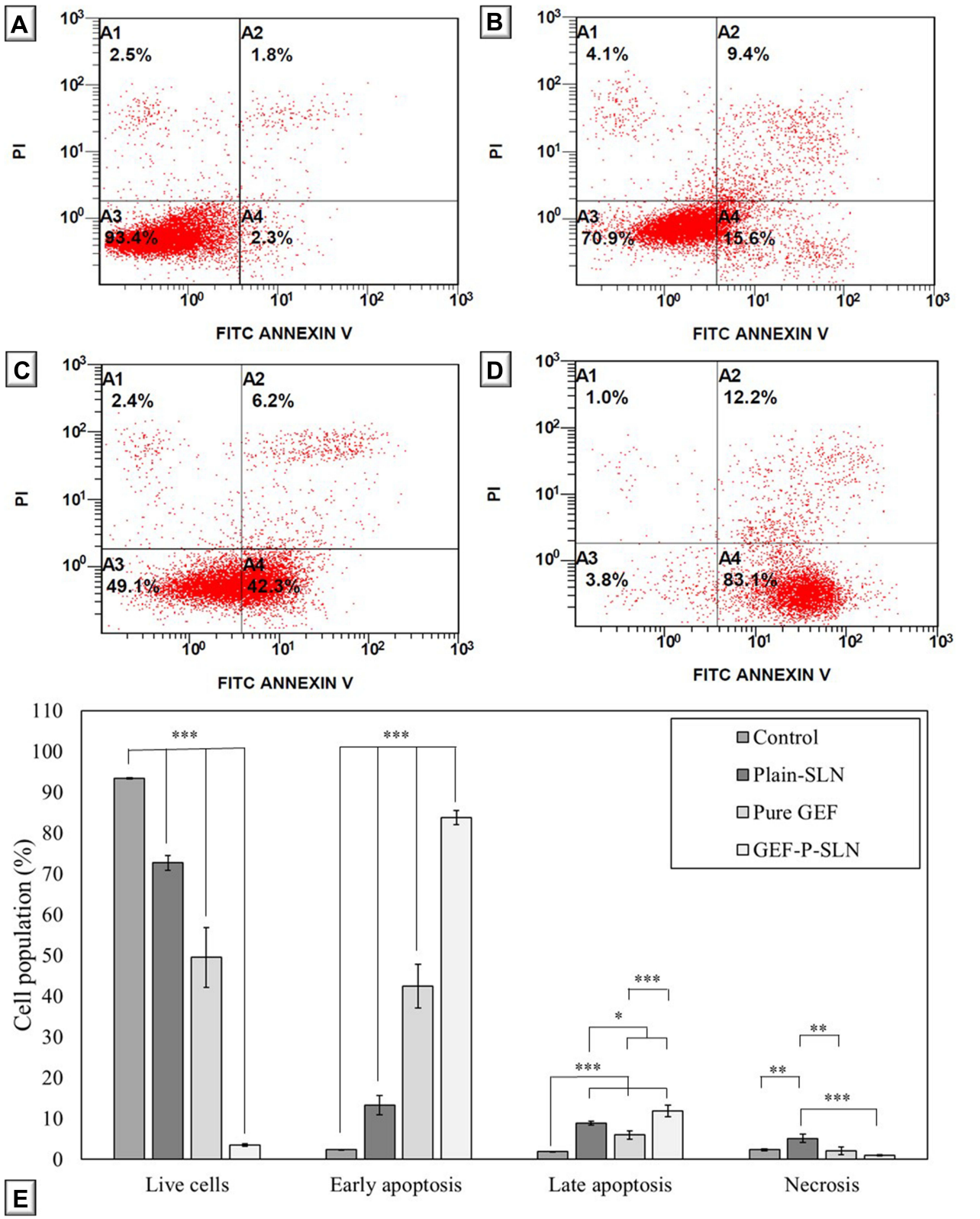

Figure 11 Flow cytometric analysis of A549 cell line treated with (**A**) Control, (**B**) Plain-SLN, (**C**) pure GEF, and (**D**) GEF-P-SLN at 3.5 μg/mL concentration. (A1, A2, A3, and A4) Necrotic, late apoptotic, early apoptotic, and viable cells are shown in the upper left quadrant, upper right quadrant, lower right quadrant, and lower left quadrant, respectively. (**E**) Bar chart shows the percentage of live, early apoptosis, late apoptosis, and necrotic cells that were treated with control, Plain-SLN, pure GEF, and GEF-P-SLN.

Notes: Data were expressed as the mean ± SD, N = 3, p-value significant at *0.05, **0.01, and ***0.001.

Abbreviations: Plain-SLN, drug-free solid lipid nanoparticle; GEF-P-SLN, gefitinib-loaded PEGylated solid lipid nanoparticle.

Table 8 Showed the Physicochemical Properties of GEF-SLN and GEF-P-SLN on 0, 7, 15, 22, and 30 Days

Characterization	PS	ZP	ZP	EE
GEF-SLN				
0 Day	324.9 ± 4.0	0.139 ± 0.051	−21.0 ± 0.9	91.2 ± 2.8
7 Days	368.6 ± 6.6	0.150 ± 0.012	−20.1 ± 1.9	85.1 ± 3.7
15 Days	401.9 ± 8.7	0.246 ± 0.046	−17.8 ± 1.4	84.2 ± 2.7
22 Days	402.7± 5.1	0.254 ± 0.015	−16.1 ± 1.6	82.8 ± 2.3
30 Days	511.0 ± 16.2	0.322 ± 0.041	−19.0 ± 1.5	77.9 ± 3.9
GEF-P-SLN				
0 Day	286.8 ± 11.8	0.124 ± 0.008	−22.3 ± 0.6	91.3 ± 2.1
7 Days	330.1 ± 1.7	0.198 ± 0.006	−18.2 ± 1.1	88.3 ± 3.4
15 Days	404.1 ± 12.3	0.289 ± 0.006	−16.4 ± 0.9	86.0 ± 4.9
22 Days	419.6 ± 9.9	0.294 ± 0.025	−16.7 ± 1.7	83.0 ± 3.2
30 Days	438.3 ± 5.4	0.277 ± 0.031	−18.5 ± 1.9	81.3 ± 3.7

Note: Data were expressed as the mean ± SD, N = 3.
Abbreviations: GEF-SLN, gefitinib-loaded solid lipid nanoparticle; GEF-P-SLN, gefitinib-loaded PEGylated solid lipid nanoparticle.

and the narrowest PDI. The former enhances the enterocyte uptake mechanism,[27] while the latter increases the physical stability of the produced SLN.[33] The slight increase in the particle size during storage could be attributed to particle aggregation.

Effect of Lipid Concentration

In agreement with the obtained results, Mahmoud et al found that decreasing SA concentration significantly decreases the PS of the obtained SLN.[34] Moreover, various studies were performed on different types of solid lipids. It was found that increasing lipid concentration resulted in a significant increase in the particle size of the prepared SLN.[10,30,33] Likewise, Nayek et al found that formulations produced from low lipid concentration had smaller PS, lower PDI, and higher ZP. This was attributed to the increasing viscosity of SLN formulation which lowers the distribution of energy during the process.[9] This resulted in reducing energy transmission during production which hinders particle size reduction; large PS, homogenous distribution of energy; high PDI value.[33]

Increasing the administered solid lipid proportion within SLN formulation (>60%) enhances entrapment efficiency,[32] stimulates bile salts secretion along with enhancing lymphatic uptake; enhances chylomicron formation,[21] and produces robust drug solubilization after dilution.[9] However, during the production of the Plain-SLN_6, a notable amount of lipid was stuck to the wall of the beaker. Besides, it was expected that most of the drug is predominantly present in solid lipid which could be lost during the production process. Furthermore, a high PDI value was observed with Plain-SLN_6 which could be attributed to the higher viscosity of the formulation. Therefore, Plain-SLN_5 was selected as the optimum formulation to avoid drug loss during the production process (occurred with Plain-SLN_6) and superior stability. During storage, a slight increase in particle size could be attributed to particle aggregation.

Effect of Surfactant Type

In harmony with the obtained results, SLN was prepared from PF-68, T-80, and PVA and it has been found that PF-68 was able to produce the smallest particles. This resulted from the thermodynamic and mechanical barrier at the boundary which prevents the coalescence of particles.[27] Likewise, Qushawy et al prepared a different SLN formulation and it has been found that PF-68 produce smaller particles than T-80.[35]

PF-68 was selected as the optimum surfactant to produce SLN. This attributed to less GEF solubility to avoid drug deposition on the surface of SLN. Moreover, PF-68 was able to produce the smallest particles with a higher degree of stability. This is attributed to the steric stabilization effect produced by PEG blocks on the surface of SLN as a result of coating influence.[9,29,30]

Effect of Surfactant Concentration

Contrasting solid lipid, increasing the concentration of surfactant did not affect the viscosity of the formulation. This resulted from its inability to affect the distribution of energy during the ultra-sonication process.[30] In harmony with the obtained results, Qushawy et al and Kumar et al found that increasing surfactant concentration leads to a decrease in PS as a result of steric stabilization produced by surfactant and prevents aggregation.[10,35]

Even though the increasing concentration of surfactant produces the smallest PS, Plain-$SLN_{10\text{-}11}$ was unstable, and aggregation was observed. This could be attributed to the presence of excess free PF-68 in the solution which deposits on the surface of SLN and facilitates particle aggregation. Even though Plain-$SLN_{5 \text{ and } 9}$ produces particles with slightly larger particles when compared with Plain-$SLN_{10\text{-}11}$, the former were selected as a result of SLN stability. Moreover, maximum stability was observed in Plain-SLN_9 which could be attributed to the balance between deposition of surfactant on SLN surface and free surfactant in nano-suspension. This occurs during the emulsification process where excess surfactants swim in the solution. In addition, the higher stability of SLN containing 1% PF-68 could result from its low PDI. Therefore, 1% of PF-68 was selected as the optimum surfactant concentration.

Effect of Solid Lipid/ Drug Ratio

Increasing the number of particles in SLN with an increasing solid lipid/drug ratio while fixing the amount of solid lipid used could result in entrapment of GEF. On the contrary, decreasing the solid lipid/drug ratio while fixing the amount of drug used increased the particle size of GEF-SLN. Therefore, two $SLN_{4 \text{ and } 6}$ were selected based on their higher drug content and to study the effect of solid lipid/drug ratio on SLN core. Therefore, they were subjected to DSC and XRD for further explanation.

DSC

The change in the melting point with an increased heated rate is expected to increase the melting points as a result of the time needed to increase the temperature of the formulation. It is expected to observe the melting point for GEF when the heating rate is increased as a result of the time needed by the formulation to acquire the energy. However, the absence of a characteristic peak of GEF even with a faster heating rate indicates either the presence of the drug in an amorphous state or the dispersion of the drug within the matrix, which facilitates solubilization before its melting. Therefore, for further investigation, the selected two formulations were subjected to further investigation with PXRD.

PXRD

The XRD measurement was performed to observe the physical state of GEF within SLN and evaluate the effect of GEF on the structural arrangement of the solid lipid (SA). It was observed that the degree and order of SA crystallinity were affected by the preparation method and storage. Raw SA has characteristic peaks with variable intensity when compared with freshly melted then cooled SA. Along with this, both GEF-SLN are characterized by the disappearance or reduction of the peak of both GEF and SA at 38.1° and 44.3. This could be attributed to the incorporation of GEF resulting in disorder in the crystallinity of SA. Furthermore, a significant reduction in the intensity of peaks with GEF-SLN_6 is expected to increase the ratio drug, which decreases the crystallinity of SA. This could be observed in the morphological appearance of freshly melted and cooled SA as well as a mixture of SA and GEF. Besides, the disappearance of characteristic peaks of GEF that are either present in amorphous form or homogenously distributed in the core of SA. Therefore, it is expected that GEF changes the crystallinity of SA.

The obtained result was in harmony with Pawar et al prepared aerosolized lipid matrix of SA containing GEF. XRD scan of the prepared drug-loaded lipid matrix shows a significant reduction in SA crystallinity.[36] Furthermore, Kumar and Randhawa found that the degree of SA crystallinity decreased after their incorporation in SLN.[37] Likewise, Dantas et al

found that incorporation of tacrolimus in SLN resulted in the loss of crystallinity of beeswax (solid lipid). This observation was confirmed by the DSC and XRD.[38] Moreover, Garg and Singh found that the crystalline peak intensity of SA significantly decreased following its incorporation in SLN.[39]

SEM

Overall, the SEM image showed particle aggregation and enlargement that could be attributed to the use of highly concentrated suspension drug preparation in the film. The change in the morphological appearance of Plain-SLN and GEF-SLN could be attributed to a change in the crystallinity of SA that was observed in PXRD. Together, SEM images of Plain-P-SLN and GEF-P-SLN showed that particles are sticky to each other. The stickiness of PEGylated SLN could be attributed to the presence of TPGS, which increases the fluidity of the SLN surface and enhances particle aggregation during dryness.

In-vitro Release

The initial drug release profile showed zero-order drug release, which indicates the erosion of the SLN shell. Therefore, all particles lost surfactants that are predominantly present on the surface of SLN. Later, the kinetic analysis of GEF released from all formulations followed the Higuchi model. This reflects either slow surface erosion of solid lipid from SLN or particle aggregation after losing surfactants with continuous drug release. Both increased the distance needed to be traveled for GEF until reaching dissolution media. GEF-SLN_6 and GEF-P-SLN showed faster and higher drug release when compared with other formulations. This could be attributed to a smaller particle size which increases the surface area and distance needed to be migrated by GEF. Therefore, GEF-SLN_6 and GEF-P-SLN were selected as optimized formulations and subjected to further evaluation. It showed be noted that GEF-SLN_6 was mentioned in the rest of the manuscript as GEF-SLN.

Ex-vivo Permeability

This experiment aims to study the permeability of GEF suspension, GEF-SLN, and GEF-P-SLN using a freshly excised rabbit intestine. The present results are in alignment with Nagaraj et al who developed SLN consisting of Dynasan118, phospholipids, and PF-68. Ex-vivo permeability across the rat intestine revealed a significant enhancement in drug permeability when compared with drug suspension.[40] Likewise, Soni et al found that the prepared lipid nanoparticles that consisted of SA as lipid phase and T-80, capryol 90, and labrasol as surfactants were able to enhance the permeability of Pemetrexed. Ex-vivo permeability study revealed that the developed formulation enhanced the drug permeability ratio by about 6-folds compared to the drug solution.[41] In addition, Neupane et al developed SLN consisting of drug conjugated SA and surfactants (PF-68, T-80, and Labrasol). It was found that SLN was able to enhance the amount of permeated drug 4-folds compared to a drug suspension. The authors referred to the presence of surfactants that enhance drug permeability and inhibit efflux transporters.[42] Regarding TPGS, Godugu et al developed a prepared solid dispersion of GEF containing TPGS using a spray drier. In-vitro permeability using Caco-2 cell lines revealed 2-fold enhancement in GEF permeability when compared with pure drug suspension.[43] Likewise, Alhowyan et al found that TPGS enhanced the intestinal permeability of fluconazole compared to drug suspension.[44] Therefore, the enhancement in GEF permeability produced by GEF-P-SLN could be attributed to the presence of TPGS which is reported to enhance the permeability of drugs susceptible to efflux transporters.[43] Therefore, the developed formulations enhanced drug permeability as a result of their nano-size and the presence of PF-68 that enhance drug permeability. Likewise, a significant enhancement in permeability was achieved via a formulation containing TPGS as a result of the efflux inhibition effect.

In-vitro Cytotoxicity

Following absorption of SLNs either through enterocytes or M cells, they are transported through LS and distributed inside the body. It has been reported that SLN consisting of SA as a lipid phase showed a higher drug distribution to lung cells following oral administration.[45] Therefore, in-vitro cytotoxicity of GEF was studied against lung cancer cells (A549) as a main site of action. In agreement with the obtained results, Zhang et al found that A549 cell lines treated with SA induced cell apoptosis and prevented cell proliferation.[46] Moreover, Öztürk et al prepared optimum SLN containing

SA and tripalmitin as a nanocarrier for clarithromycin. An in-vitro cytotoxicity study revealed that IC_{50} for Plain-SLN was 8 μg/mL.[31] The low cytotoxic activity of pure GEF is attributed to the susceptibility of GEF to efflux transporters at lower concentrations.[18] On the other hand, the abundance of GEF at higher concentrations exceeds the capacity of efflux transporters that enhance its cytotoxic effect. The enhancement in GEF cytotoxic effect for both formulations at low concentrations (2.5 and 5 μg/mL) could be attributed to enhancement in the cellular uptake. It has been proved that encapsulation of therapeutic agents with nanoparticles improves cellular internalization and consequently cytotoxic effect.[9] In addition, the presence of PF-68 in both formulations could enhance the cellular internalization of GEF by preventing efflux transporters.[47] Additionally, the presence of TPGS in GEF-P-SLN augments efflux transporters' inhibition activity produced by PF-68.[48] This could be observed from a significant enhancement in cell death activity at lower concentrations (2.5 and 5 μg/mL) and lower IC_{50} for GEF-P-SLN when compared with GEF-SLN. Accordingly, GEF-P-SLN was selected for further investigation.

Apoptosis Study

Apoptosis is a complex physiological process initiated to eliminate and remove unwanted cells from the body. Therefore, an apoptotic study is used to quantify and sort the population of cells based on their stages after treatment with a drug or formulation.[49] The obtained results confirmed that the presence of PF-68 and TPGS enhanced the bioactivity of GEF. This is achieved through the enhancement of drug internalization and preventing its efflux from the cytoplasm toward outside cells. Hence, GEF-P-SLN could enhance the apoptotic activity of the drug as a result of previously described mechanisms. This reduces the required dose to achieve the optimum therapeutic drug level that in turn decreases the side effects and toxicity of GEF.

The obtained results were in harmony with Hu et al who developed a lipid-based formulation to enhance the apoptotic activity of GEF. The apoptotic study showed that A549 cells stages following treatment with GEF-loaded liposomes at early and late apoptosis stages when compared with pure GEF.[50] Likewise, Pang et al found that albumin nanoparticles loaded with GEF increase the early and late apoptosis of NCI–H358 cell line when compared with pure GEF.[51] In alignment with the proposed hypothesis, Wang et al developed SLN consisting of stearic acid as a lipid phase for the treatment of lung cancer. The biodistribution study showed that higher drug concentration was detected in lung tissue.[45]

Practically, conventional administration of GEF resulted in poor therapeutic outcomes when used at lower concentrations.[18] This is attributed to low drug distribution and susceptibility to resistance mechanisms, such as efflux transporters.[15] For this purpose, high doses of chemotherapeutic agents are administered to patients, which causes high systemic toxicity. Therefore, enhancing the cytotoxic effect of administered chemotherapeutic agent decreases the required therapeutic response besides low side effects.[9] Along with that, encapsulation of therapeutic agents within an appropriate lipoprotein mimic carrier enhances cellular uptake and lung biodistribution.[45] This prevents GEF from binding to plasma proteins, which increases the percentage of a free drug for biodistribution.[15] Therefore, herein the developed GEF-P-SLN enhances the cytotoxic activity of GEF at lower concentrations with a highly desirable biodistribution outcome.

Stability Study

Even though the particle size of the prepared GEF-SLN and GEF-P-SLN was increased, it is still in the nanosize range. This could be attributed to particle aggregation during storage. The reduction in the EE of GEF could be attributed to changes in the crystallinity of SA during storage. This outcome follows a PXRD study that showed changes in SA crystallization during storage. This change in crystallinity resulted in the explosion of GEF from the core of SLN.

Conclusion

In the current study, the effect of solid lipid and surfactant type, as well as their concentration, was evaluated to prepare SLN with desirable physicochemical properties and stability. It was found that decreasing degree of glycerol esterification and lipid content produced SLN with low particle size. Furthermore, increasing the HLB value of the used surfactant and its concentration resulted in decreasing particle size of SLN. Additionally, the effect of drug loading on the physicochemical properties was evaluated to prepare GEF-SLN and GEF-P-SLN. The prepared GEF-

SLN and GEF-P-SLN are in the nanosize range, and homogenous with a negative ZP value. DSC and PXRD showed that GEF affected the crystallinity of stearic acid and the drug was present in the amorphous state. Also, they showed remarkable EE of GEF and exhibited a sustained-release profile over 24 hrs. The GEF-SLN and GEF-P-SLN augmented the permeability of the GEF through the rabbit intestine compared with GEF suspension. Furthermore, GEF-P-SLN enhanced the cytotoxicity and apoptotic effect of GEF against A549 as a model for lung cancer. The obtained GEF-P-SLN follows the LDD criteria due to lipid nature, nanosize, and negative ZP. The presence of SA in GEF-P-SLN might increase drug targeting to the lung cells. This indicated that GEF-P-SLN is a promising approach to improving therapeutic outcomes of GEF in the treatment of metastatic lung cancers. Furthermore, in vivo studies are required to address the impact of the developed P-SLN on the LDD of GEF using the animal model for lung cancer.

Abbreviations

7LS, lymphatic system; LDD, lymphatic drug delivery; GEF, gefitinib; EGFR, epidermal growth factor receptors; PS, particle size; ZP, zeta potential; PDI, polydispersity index.

Institutional Review Board Statement

All experimental protocols were approved by the Research Ethics Committee (REC) (Ethics reference number: KSU-SE -22-15) at King Saud University, Al-Riyadh, Saudi Arabia. The procedure followed the guidelines set by the Animal Care and Use Committee of our institute and the National Institutes of Health.

Data Sharing Statement

The data that support the findings of this study are available from the corresponding author, upon reasonable request.

Funding

The authors extend their appreciation to the Deanship of Scientific Research, King Saud University for funding through Vice Deanship of Scientific Research Chairs, Kayyali Chair for Pharmaceutical Industry, Department of Pharmaceutics, College of Pharmacy, for funding the work through Grant Number AG-2022.

Disclosure

The authors report no conflicts of interest in this work.

References

1. World Health Organization. Cancer; 2021. Available from: https://www.who.int/news-room/fact-sheets/detail/cancer. Accessed January 10, 2022.
2. Thandra KC, Barsouk A, Saginala K, Aluru JS, Barsouk A. Epidemiology of lung cancer. *Contemp Oncol*. 2021;25(1):45. doi:10.5114/wo.2021.103829
3. Mousapasandi A, Loke WSJ, Herbert CA, Thomas PS. Oxidative stress in lung cancer. In: *Cancer*. Elsevier; 2021:27–37.
4. Miao YB, Lin YJ, Chen KH, et al. Engineering nano-and microparticles as oral delivery vehicles to promote intestinal lymphatic drug transport. *Adv Mater*. 2021;33(51):2104139. doi:10.1002/adma.202104139
5. Chaturvedi S, Verma A, Saharan VA. Lipid drug carriers for cancer therapeutics: an insight into lymphatic targeting, P-gp, CYP3A4 modulation and bioavailability enhancement. *Adv Pharma Bull*. 2020;10(4):524. doi:10.34172/apb.2020.064
6. Li Z, Yang E, Long X. Function of the lymphatic system. In: *Peripheral Lymphedema*. Springer; 2021:45–48.
7. Sharma JB, Bhatt S, Saini V, Kumar M. Pharmacokinetics and pharmacodynamics of curcumin-loaded solid lipid nanoparticles in the management of streptozotocin-induced diabetes mellitus: application of central composite design. *Assay Drug Dev Technol*. 2021;19(4):262–279. doi:10.1089/adt.2021.017
8. Vishwakarma N, Jain A, Sharma R, Mody N, Vyas S, Vyas SP. Lipid-based nanocarriers for lymphatic transportation. *AAPS PharmSciTech*. 2019;20(2):1–13. doi:10.1208/s12249-019-1293-3
9. Nayek S, Raghavendra N, Kumar BS. Development of novel S PC-3 gefitinib lipid nanoparticles for effective drug delivery in breast cancer. Tissue distribution studies and cell cytotoxicity analysis. *J Drug Deliv Sci Technol*. 2021;61:102073. doi:10.1016/j.jddst.2020.102073
10. Kumar S, Narayan R, Ahammed V, Nayak Y, Naha A, Nayak UY. Development of ritonavir solid lipid nanoparticles by Box Behnken design for intestinal lymphatic targeting. *J Drug Deliv Sci Technol*. 2018;44:181–189. doi:10.1016/j.jddst.2017.12.014
11. Khutoryanskiy VV. Beyond PEGylation: alternative surface-modification of nanoparticles with mucus-inert biomaterials. *Adv Drug Deliv Rev*. 2018;124:140–149. doi:10.1016/j.addr.2017.07.015

12. Rathod S, Bahadur P, Tiwari S. Nanocarriers based on vitamin E-TPGS: design principle and molecular insights into improving the efficacy of anticancer drugs. *Int J Pharm*. 2021;592:120045. doi:10.1016/j.ijpharm.2020.120045
13. Fine-Shamir N, Beig A, Dahan A. Adequate formulation approach for oral chemotherapy: etoposide solubility, permeability, and overall bioavailability from cosolvent-vs. vitamin E TPGS-based delivery systems. *Int J Pharm*. 2021;597:120295. doi:10.1016/j.ijpharm.2021.120295
14. Zhang L, Li N, Liu M, Zheng B, Wu Z, Cai H. Cost-effectiveness analysis of dacomitinib versus gefitinib in the first-line treatment of EGFR-positive advanced or metastatic non-small cell lung cancer. *Cancer Manag Res*. 2021;13:4263. doi:10.2147/CMAR.S293983
15. Makeen HA, Mohan S, Al-Kasim MA, et al. Gefitinib loaded nanostructured lipid carriers: characterization, evaluation and anti-human colon cancer activity in vitro. *Drug Deliv*. 2020;27(1):622–631. doi:10.1080/10717544.2020.1754526
16. Nayek S, Raghavendra N, Kumar BS. Development of novel S PC-3 gefitinib lipid nanoparticles for effective drug delivery in breast cancer. Tissue distribution studies and cell cytotoxicity analysis. *J Drug Deliv Sci Technol*. 2020;61:102073.
17. Shao J, Xu Z, Peng X, et al. Gefitinib synergizes with irinotecan to suppress hepatocellular carcinoma via antagonizing Rad51-mediated DNA-repair. *PLoS One*. 2016;11(1):e0146968. doi:10.1371/journal.pone.0146968
18. Wang J, Wang F, Li X, Zhou Y, Wang H, Zhang Y. Uniform carboxymethyl chitosan-enveloped Pluronic F68/poly (lactic-co-glycolic acid) nano-vehicles for facilitated oral delivery of gefitinib, a poorly soluble antitumor compound. *Colloids Surf B Biointerfaces*. 2019;177:425–432. doi:10.1016/j.colsurfb.2019.02.028
19. Liu G, Lin Q, Huang Y, Guan G, Jiang Y. Tailoring the particle microstructures of gefitinib by supercritical CO2 anti-solvent process. *J CO2 Util*. 2017;20:43–51. doi:10.1016/j.jcou.2017.04.015
20. Bhalekar MR, Madgulkar AR, Desale PS, Marium G. Formulation of piperine solid lipid nanoparticles (SLN) for treatment of rheumatoid arthritis. *Drug Dev Ind Pharm*. 2017;43(6):1003–1010. doi:10.1080/03639045.2017.1291666
21. Patel P, Patel M. Enhanced oral bioavailability of nintedanib esylate with nanostructured lipid carriers by lymphatic targeting: in vitro, cell line and in vivo evaluation. *Eur J Pharma Sci*. 2021;159:105715. doi:10.1016/j.ejps.2021.105715
22. Harisa GI, Badran MM. Simvastatin nanolipid carriers decreased hypercholesterolemia induced cholesterol inclusion and phosphatidylserine exposure on human erythrocytes. *J Mol Liq*. 2015;208:202–210. doi:10.1016/j.molliq.2015.04.005
23. Alshehri S, Alanazi A, Elzayat EM, et al. Formulation, in vitro and in vivo evaluation of gefitinib solid dispersions prepared using different techniques. *Processes*. 2021;9(7):1210. doi:10.3390/pr9071210
24. Baek J-S, Cho C-W. Surface modification of solid lipid nanoparticles for oral delivery of curcumin: improvement of bioavailability through enhanced cellular uptake, and lymphatic uptake. *Eur J Pharma Biopharma*. 2017;117:132–140. doi:10.1016/j.ejpb.2017.04.013
25. Srinivas NSK, Verma R, Kulyadi GP, Kumar L. A quality by design approach on polymeric nanocarrier delivery of gefitinib: formulation, in vitro, and in vivo characterization. *Int J Nanomedicine*. 2017;12:15. doi:10.2147/IJN.S122729
26. Nasr FA, Noman OM, Alqahtani AS, et al. Phytochemical constituents and anticancer activities of Tarchonanthus camphoratus essential oils grown in Saudi Arabia. *Saudi Pharma J*. 2020;28(11):1474–1480. doi:10.1016/j.jsps.2020.09.013
27. Sharma M, Gupta N, Gupta S. Implications of designing clarithromycin loaded solid lipid nanoparticles on their pharmacokinetics, antibacterial activity and safety. *RSC Adv*. 2016;6(80):76621–76631. doi:10.1039/C6RA12841F
28. Dhairyasheel G, Adhikrao Y, Varsha G. Design and development of solid self-microemulsifying drug delivery of gefitinib. *Asian J Pharm Technol*. 2018;8(4):193–199. doi:10.5958/2231-5713.2018.00031.4
29. Zardini AA, Mohebbi M, Farhoosh R, Bolurian S. Production and characterization of nanostructured lipid carriers and solid lipid nanoparticles containing lycopene for food fortification. *J Food Sci Technol*. 2018;55(1):287–298. doi:10.1007/s13197-017-2937-5
30. Khalil RM, Abd El-Bary A, Kassem MA, Ghorab MM, Ahmed MB. Solid lipid nanoparticles for topical delivery of meloxicam: development and in vitro characterization. *Eur Scientific J*. 2013;9(21):45.
31. Öztürk AA, Aygül A, Şenel B. Influence of glyceryl behenate, tripalmitin and stearic acid on the properties of clarithromycin incorporated solid lipid nanoparticles (SLNs): formulation, characterization, antibacterial activity and cytotoxicity. *J Drug Deliv Sci Technol*. 2019;54:101240. doi:10.1016/j.jddst.2019.101240
32. Das S, Ng WK, Kanaujia P, Kim S, Tan RB. Formulation design, preparation and physicochemical characterizations of solid lipid nanoparticles containing a hydrophobic drug: effects of process variables. *Colloids Surf B Biointerfaces*. 2011;88(1):483–489. doi:10.1016/j.colsurfb.2011.07.036
33. Rigon RB, Gonçalez ML, Severino P, et al. Solid lipid nanoparticles optimized by 22 factorial design for skin administration: cytotoxicity in NIH3T3 fibroblasts. *Colloids Surf B Biointerfaces*. 2018;171:501–505. doi:10.1016/j.colsurfb.2018.07.065
34. Mahmoud RA, Hussein AK, Nasef GA, Mansour HF. Oxiconazole nitrate solid lipid nanoparticles: formulation, in-vitro characterization and clinical assessment of an analogous loaded carbopol gel. *Drug Dev Ind Pharm*. 2020;46(5):706–716. doi:10.1080/03639045.2020.1752707
35. Qushawy M, Prabahar K, Abd-Alhaseeb M, Swidan S, Nasr A. Preparation and evaluation of carbamazepine solid lipid nanoparticle for alleviating seizure activity in pentylenetetrazole-kindled mice. *Molecules*. 2019;24(21):3971. doi:10.3390/molecules24213971
36. Pawar AA, Chen D-R, Venkataraman C. Influence of precursor solvent properties on matrix crystallinity and drug release rates from nanoparticle aerosol lipid matrices. *Int J Pharm*. 2012;430(1–2):228–237. doi:10.1016/j.ijpharm.2012.03.030
37. Kumar S, Randhawa JK. Solid lipid nanoparticles of stearic acid for the drug delivery of paliperidone. *RSC Adv*. 2015;5(84):68743–68750. doi:10.1039/C5RA10642G
38. Dantas IL, Bastos KTS, Machado M, et al. Influence of stearic acid and beeswax as solid lipid matrix of lipid nanoparticles containing tacrolimus. *J Therm Anal Calorim*. 2018;132(3):1557–1566. doi:10.1007/s10973-018-7072-7
39. Garg A, Singh S. Enhancement in antifungal activity of eugenol in immunosuppressed rats through lipid nanocarriers. *Colloids Surf B Biointerfaces*. 2011;87(2):280–288. doi:10.1016/j.colsurfb.2011.05.030
40. Nagaraj B, Tirumalesh C, Dinesh S, Narendar D. Zotepine loaded lipid nanoparticles for oral delivery: development, characterization, and in vivo pharmacokinetic studies. *Future J Pharma Sci*. 2020;6(1):1–11. doi:10.1186/s43094-020-00051-z
41. Soni K, Mujtaba A, Kohli K. Lipid drug conjugate nanoparticle as a potential nanocarrier for the oral delivery of pemetrexed diacid: formulation design, characterization, ex vivo, and in vivo assessment. *Int J Biol Macromol*. 2017;103:139–151. doi:10.1016/j.ijbiomac.2017.05.015
42. Neupane YR, Sabir M, Ahmad N, Ali M, Kohli K. Lipid drug conjugate nanoparticle as a novel lipid nanocarrier for the oral delivery of decitabine: ex vivo gut permeation studies. *Nanotechnology*. 2013;24(41):415102. doi:10.1088/0957-4484/24/41/415102
43. Godugu C, Doddapaneni R, Patel AR, Singh R, Mercer R, Singh M. Novel gefitinib formulation with improved oral bioavailability in treatment of A431 skin carcinoma. *Pharm Res*. 2016;33(1):137–154. doi:10.1007/s11095-015-1771-6

44. Alhowyan AA, Altamimi MA, Kalam MA, et al. Antifungal efficacy of Itraconazole loaded PLGA-nanoparticles stabilized by vitamin-E TPGS: in vitro and ex vivo studies. *J Microbiol Methods*. 2019;161:87–95. doi:10.1016/j.mimet.2019.01.020
45. Wang P, Zhang L, Peng H, Li Y, Xiong J, Xu Z. The formulation and delivery of curcumin with solid lipid nanoparticles for the treatment of on non-small cell lung cancer both in vitro and in vivo. *Mater Sci Eng C*. 2013;33(8):4802–4808. doi:10.1016/j.msec.2013.07.047
46. Zhang L, Lv J, Chen C, Wang X. Roles of acyl-CoA synthetase long-chain family member 5 and colony stimulating factor 2 in inhibition of palmitic or stearic acids in lung cancer cell proliferation and metabolism. *Cell Biol Toxicol*. 2021;37(1):15–34. doi:10.1007/s10565-020-09520-w
47. Shah P, Chavda K, Vyas B, Patel S. Formulation development of linagliptin solid lipid nanoparticles for oral bioavailability enhancement: role of P-gp inhibition. *Drug Deliv Transl Res*. 2021;11(3):1166–1185. doi:10.1007/s13346-020-00839-9
48. Tanaudommongkon I, Tanaudommongkon A, Prathipati P, Nguyen JT, Keller ET, Dong X. Curcumin nanoparticles and their cytotoxicity in docetaxel-resistant castration-resistant prostate cancer cells. *Biomedicines*. 2020;8(8):253. doi:10.3390/biomedicines8080253
49. Wang C, Cui C. Inhibition of lung cancer proliferation by wogonin is associated with activation of apoptosis and generation of reactive oxygen species. *Balkan Med j*. 2020;37(1):29.
50. Hu Y, Zhang J, Hu H, Xu S, Xu L, Chen E. Gefitinib encapsulation based on nano-liposomes for enhancing the curative effect of lung cancer. *Cell Cycle*. 2020;19(24):3581–3594. doi:10.1080/15384101.2020.1852756
51. Pang X, Yang P, Wang L, et al. Human serum albumin nanoparticulate system with encapsulation of gefitinib for enhanced anti-tumor effects in non-small cell lung cancer. *J Drug Deliv Sci Technol*. 2019;52:997–1007. doi:10.1016/j.jddst.2019.06.011